RS

Radiology Study

Learn and upturn.

1

April 2019

Radiology Study

Web:

www.radiologystudy.ru

E-Mail:

a.e.nikolaev@yandex.ru

RS-journal@yandex.ru

RS – electronic periodical about Diagnostic Radiology

Publication frequency: 4 issues per year (quarterly).

Language: English and Russian

Logo, cover, website design: Nikolaev Alexander

Dear friends and colleagues!

We are glad to present the first issue of our journal in a completely new format. In this issue, a large number of articles and interesting cases from practice dedicated on different radiologic sub-specialisation.

We believe that readers will find in this issue materials that will answer their questions and help in practical work. We are waiting for your letters with questions and suggestions on the subject of the following issues.

radiologystudy.ru -
Learn and upturn

Radiology Study

Radiology Study is the journal publishes relevant scientific articles on radiology, radionuclide diagnostics, ultrasound diagnostics and interventional radiology, including endovascular technologies, as well as other relevant areas of medical imaging and radiotherapy.

The electronic format of the journal provides wide availability of the publication, consistently high quality of illustrative material, the ability to place DICOM files of your cases. Each issue of the journal contains articles from leading specialists in radiology.

Languages: English and Russian.

Publication frequency: 4 issues per year (quarterly).

The Journal is distributed free of charge.
Available in Russia and all over the world.

The Editorial Board of Radiology Study supports the policy aimed at compliance with all principles of publishing ethics. The ethical rules and norms correspond to those adopted by the leading international scientific publishers.

All submitted materials are subject to mandatory double-blind peer review.
The certificate of registration of mass media: El no. FS77-74575 - 14 December 2018.

Address for correspondence: RS-journal@yandex.ru

All materials for publication in the journal are sent to this address.

radiologystudy.ru - Learn and upturn

Editorial board:

Address of the journal: radiologystudy.ru

Address for correspondence: a.e.nikolaev@yandex.ru

Registration number: El no. FS77-74575 dated 14 December 2018

Founder: Alexander E. Nikolaev

Content

RS - Science Article

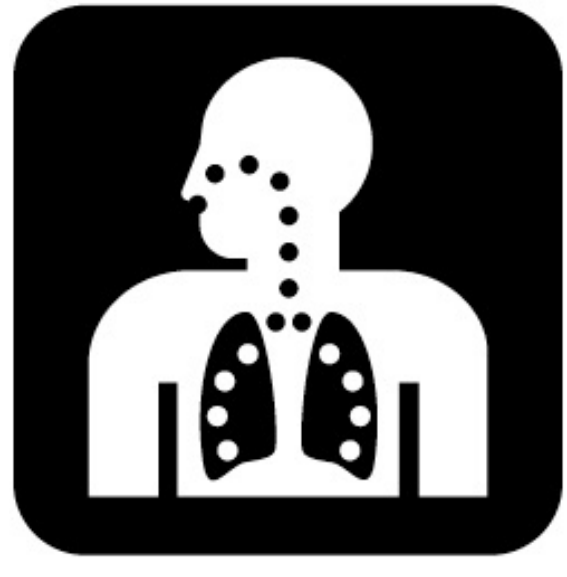

Science articles:

ARTICLE TITLE: Incidental findings of the thyroid gland on PET-CT.

AUTHORS: Suchilova M.M.1, Korkunova O. A.1, Nikolaev A. E.2, Grishkov S.M.2., Bosin V.Yu.2.

INSTITUTIONS:

1. FSBEI FPE RMACPE MOH, Russia
2. Research and Practical Clinical Center of Diagnostics and Telemedicine Technologies, Department of Health Care of Moscow, Russia

THESIS:

Incidental findings of the thyroid gland are common on the whole-body FDG (18F-flurodeoxyglucose) positron emission tomography-computed tomography (PET-CT).

Materials and Methods

A retrospective review of 100 patients with breast cancer (AJCC IV) was done. PET-CT studies with incidental focal and diffuse FDG thyroid uptake formed the review basis. These studies were performed within a period of 12 months (January 1, 2016-December 31, 2016). Twenty two (n=22) patients out of 100 (22%) had FDG thyroid uptake and comprised the study group. We excluded patients who had a history of previous thyroid malignancy or predisposing causes (e.g., Cowden syndrome).

Scans were acquired approximately 60 min after the injection of 555MBq (15mCi) FDG with the Gemini TF PET/CT (Philips Medical Systems, Cleveland, Ohio, USA) scanner with a 16-slice Brilliance CT.

Results

This study shows that thyroid FDG uptake, incidentally identified on PET/CT of patients with breast cancer (AJCC - IV), occurred at a frequency of 22%. Focal and diffuse types of uptake were diagnosed with equal frequency.

Conclusion:

However, well-defined criteria for evaluating thyroid incidentalomas on PET examinations aren’t developed yet and ultrasound still remains the method of choice for analyzing thyroid changes

KEYWORDS: incidentaloma, PET-CT, thyroid gland, FDG-uptake, petoma

CORRESPONDING AUTHOR: Suchilova M.M.

E-MAIL: maria.suchilova@gmail.com

FOR CITATIONS: Suchilova M. M.1. Korkunova O. A.1. Nikolayev A.E.2. Grishkov S.M.2. Bosin V.Yu.2. - Incidental findings of the thyroid gland on PET-CT // Radiology Study. - 2019. - T1., №1. - p.7-15

Introduction

Incidental findings of the thyroid gland are common on the whole-body FDG (18F-flurodeoxyglucose) positron emission tomography-computed tomography (PET-CT). FDG accumulates slightly in normal thyroid tissue on the whole-body PET-CT with FDG and an increase of uptake is common for pathological changes [1].

Incidental thyroid activity on FDG-PET, performed in patients without thyroid malignancy, referred to as a "PEToma" or incidentaloma. It is suggested, that such lesions are associated with a significant incidence of primary thyroid cancer over the past 20-30 years and the development of new diagnostic techniques such as PET [2].

Different studies shows that thyroid FDG uptake incidentally identified on PET-CT occurred at a frequency of 2-10%. Focal and diffuse types of uptake were diagnosed with equal frequency [1, 2]. The risk of malignancy varies: it is higher in cases with focal thyroid FDG uptake, whereas diffuse thyroid FDG uptake most likely represents chronic thyroiditis.

SUV (standardized uptake value) is usually used for distinguishing between benign and malignant thyroid PETomas. [1, 2] This parameter is considered to be high when the lesion is malignant, however, in practice it is not always the case. For example, a Hürthle adenoma has a SUVmax of 8.9, while a papillary thyroid carcinoma - only 2.8 [4]. However, well-defined criteria for evaluating thyroid incidentalomas on PET examinations aren't developed yet and ultrasound still remains the method of choice for analyzing thyroid changes [3].

Materials and Methods

A retrospective review of 100 patients with breast cancer (AJCC IV) was done. PET-CT studies with incidental focal and diffuse FDG thyroid uptake formed the review basis. These studies were performed within a period of 12 months (January 1, 2016-December 31, 2016).

Twenty two (n=22) patients out of 100 (22%) had FDG thyroid uptake and comprised the study group. We excluded patients who had a history of previous thyroid malignancy or predisposing causes (e.g., Cowden syndrome). These 22 patients were further evaluated to determine the clinical significance of unexpected focal and diffuse FDG uptake in the thyroid gland. All the patients were women in the age group of 70-75 .

18F-flurodeoxyglucose-PET/CT

Patients fasted for at least 4 hours before PET/CT imaging and had a measured finger stick glucose level less than 11.1 mmol/L (200 mg/dl) before the administration of FDG. Scans were acquired approximately 60 min after the injection of 555MBq (15mCi) FDG with the Gemini TF PET/CT (Philips Medical Systems, Cleveland, Ohio, USA) scanner with a 16-

slice Brilliance CT. Low-dose CT with contrast enhanced in arteriovenous equilibrium phase was performed.

Results

Patients, who had unexpected FDG uptake in the thyroid gland, were divided into two groups: diffuse uptake group (n=15) and focal uptake group (n=11). 4 patients had both diffuse and focal changes. Location of the focal thyroid lesions are given in Table 1.

Table 1. Location of thyroid PETomas

Location of thyroid PEToma	**N and %**
Left lobe (the largest node)	41%
Right lobe (the largest node)	59%
Istmus	9%
Bilateral	27.2%

Mean age of the patients was 73, standard deviation was ± 1,9. We correlated SUV values with focal and diffuse types of uptake (Table 2).

Table 2. SUVmax and SUVmean according to the type of uptake

	Focal FDG Uptake - min value	**Focal FDG Uptake - max value**	**Diffuse FDG Uptake - min value**	**Diffuse FDG Uptake - max value**
SUV max	1,8	13,3	1,1	8,7
SUV mean	4,2	7,0	2,2	3,4

Diffusal uptake is associated with the increased volume of the thyroid gland, however, the mean volume of the gland is also increases when uptake is focal (Table3).

Table 3. Volumes of the thyroid gland according to the type of uptake

	Focal FDG Uptake	**Percentage of normal value (upper limit)**	**Diffuse FDG Uptake**	**Percentage of normal value (upper limit)**
Mean volume of the right lobe	18,1	243%	26,6	354,7%

Mean volume of the left lobe (ml)	16,9	225,3%	20,9	278,7%
Mean total thyroid volume (ml)	34,9	232,6%	46,1	325,4%

The results of the audit demonstrate how often radiologists missed incidental findings of the thyroid gland and forgot to recommend ultrasound evaluation (Table 4).

Table 4. Results of the audit

Radiologists' mistakes	**Frequency**
Missed focal changes of the thyroid gland	30,30%
Missed diffuse changes of the thyroid gland	45,45%
Forgot to recommend ultrasound evaluation	60,60%
The thyroid gland volume is not mentioned	100%

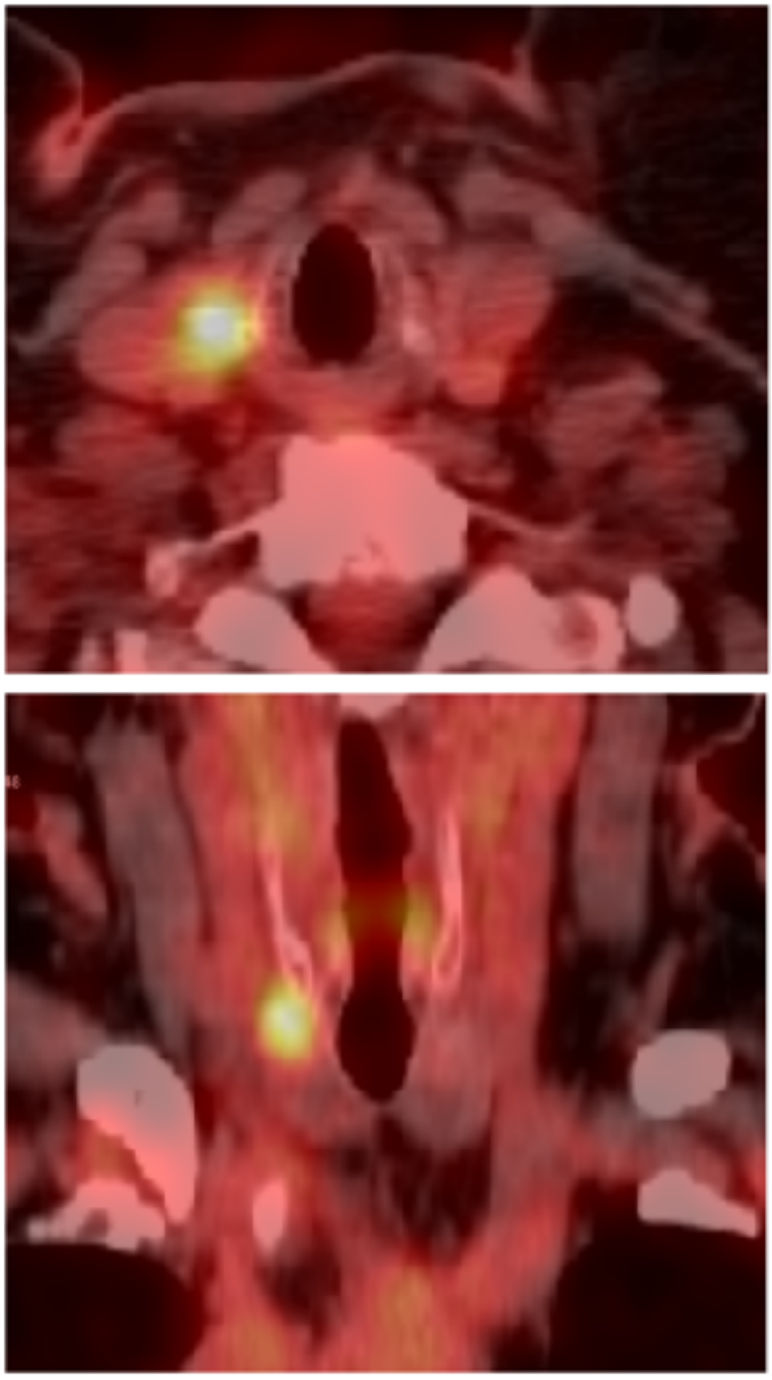

Figure 1 (a, b). The thyroid gland (axial - a, and coronal - b) with focal FDG uptake on PET-CT of the neck region

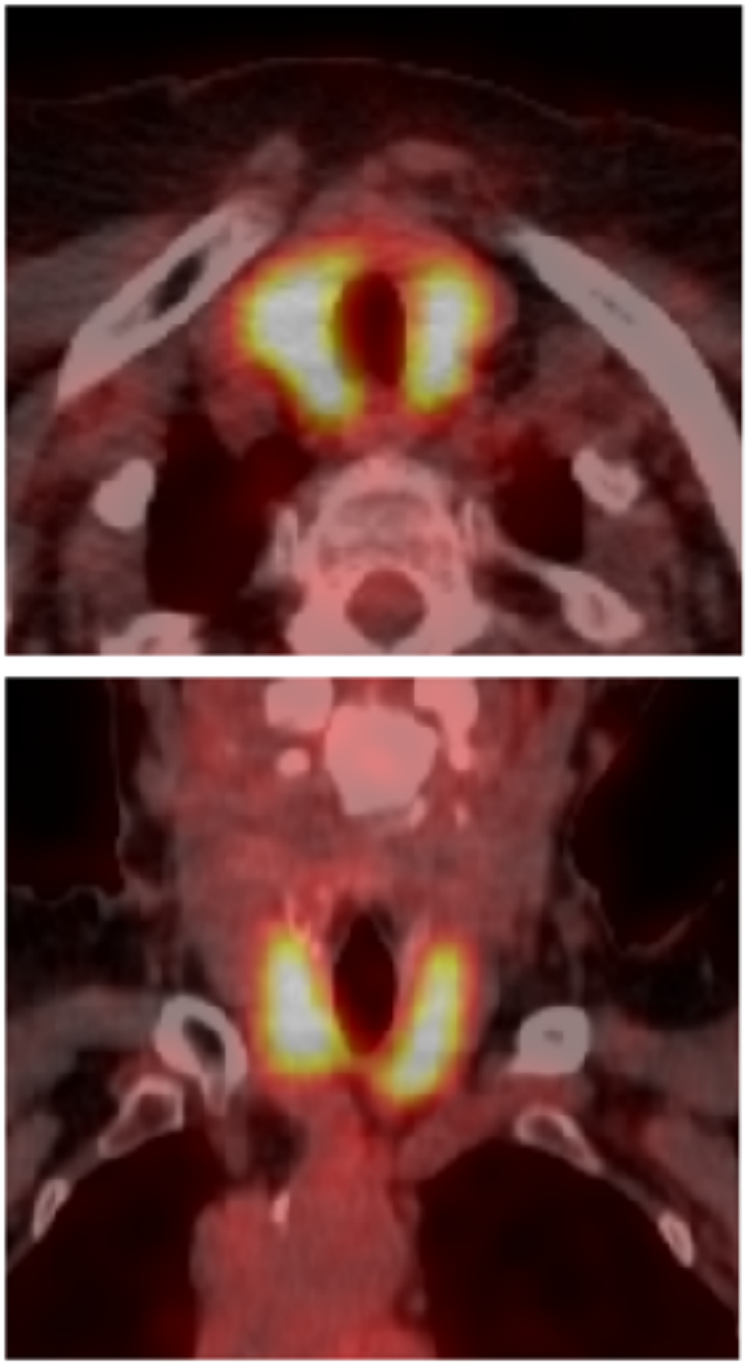

Figure 2 (a, b). The thyroid gland (axial - a, and coronal - b) with diffuse FDG uptake on PET-CT of the neck region

Discussion

In our study we retrospectively reviewed all the 100 whole-body FDG PET-CT studies performed with the aim to evaluate the prevalence of incidental FDG uptake in the thyroid gland.

Our data showed a 22% prevalence of incidental thyroid FDG uptake on FDG PET-CT and this data correlate with the literature [5, 6]. Lesions had both diffuse (15 of 22, 68%) and focal (11 of 22, 50%) uptake and more often focal uptake was in the right lobe.

Considering that the study group was small, more findings are needed to evaluate the role of SUV in the differentiation between benign and malignant lesions of the thyroid gland, that were accidentally found on PET and verified with ultrasound and biopsy. Benign lesions sometimes have much higher SUV value than malignant lesions, so quantitative evaluation of metabolic activity is not accurate thus far [4]. Ultrasound still remains the method of choice for evaluation of a thyroid incidentalomas. This method is available and cheap thuswise the evaluation of the role of SUV is not the task of prime importance.

Volume of the thyroid gland was measured in order to compare with normal female thyroid gland volume, which is ~ 10-15 ml [7]. Enlargement of the thyroid gland is nearly always seen in patients with diffuse diseases, cases with autoimmune hypothyroidism are sometimes the exception [8]. In our study, diffuse FDG uptake is seen in the enlarged thyroid gland, however, the mean volume of the gland was also increased in approximately two times, when uptake was focal.

The audit, mentioned in this study, showed weak awareness of radiologists about thyroid pathology defined on PET-CT. The results of the audit revealed that even in cases, when the changes of the thyroid gland was protocoled, thyroid volume was not mentioned and ultrasound evaluation was not recommended.

Conclusion

This study shows that thyroid FDG uptake, incidentally identified on PET/CT of patients with breast cancer (AJCC - IV), occurred at a frequency of 22%. Focal and diffuse types of uptake were diagnosed with equal frequency.

The risk of malignancy is high in lesions with focal thyroid FDG uptake, but radiologists didn’t always pay due attention to these important incidental findings and didn’t recommend ultrasound evaluation.

Diffuse thyroid FDG uptake most likely represents chronic thyroiditis and other diffuse pathologies of the thyroid gland, clinically presented with a goiter. It is important to measure the thyroid volume, because focal changes also result in gland enlargement.

Conflict of Interests.

The authors state that they have no conflict of interests.

References:

[1] - Nakamoto Y, Tatsumi M, Hammoud D, Cohade C, Osman MM, Wahl RL. Normal FDG distribution patterns in the head and neck: PET/CT evaluation. Radiology 2005; 234:879–885.

[2] - Evaluation of thyroid FDG uptake incidentally identified on FDG-PET/CT imaging Wengen Chen;Molly Parsons;Drew Torigian;Hongming Zhuang;Abass Alavi; Nuclear Medicine Communications. 30(3):240-244, MAR 2009 DOI: 10.1097/MNM. 0b013e328324b431 , PMID: 19262287 Issn Print: 0143-3636 Publication Date: 2009/03/01

[3] - Tessler FN, Middleton WD, Grant EG, Hoang JK, Berland LL, et al. ACR Thyroid Imaging, Reporting and Data System (TI-RADS): White Paper of the ACR TI-RADS Committee. (2017) Journal of the American College of Radiology : JACR. 14 (5): 587-595. doi:10.1016/j.jacr.2017.01.046 - Pubmed

[4] - Radiol Oncol. 2015 Jun; 49(2): 121–127. Published online 2015 Mar 25. doi: 10.2478/ raon-2014-0039 PMCID: PMC4387987 PMID: 26029022 Thyroid lesions incidentally detected by 18F-FDG PET-CT — Jan Jamsek, Ivana Zagar, Simona Gaberscek, and Marko Grmek

[5] - Otolaryngol Head Neck Surg. 2018 Mar;158(3):484-488. doi: 10.1177/0194599817742579. Epub 2017 Nov 21. Incidental Findings on FDG PET/CT in Head and Neck Cancer. Britt CJ1, Maas AM2, Kennedy TA3, Hartig GK2.

[6] - Eur Arch Otorhinolaryngol. 2019 Jan;276(1):243-247. doi: 10.1007/s00405-018-5203-1. Epub 2018 Dec 10. Incidental findings on 18-FDG PET-CT in head and neck cancer. A retrospective case-control study of incidental findings on 18-FDG PET-CT in patients with head and neck cancer. Casselden E1, Sheerin F2, Winter SC3,4.

[7] - Indian J Endocrinol Metab. 2013 Mar-Apr; 17(2): 219–227. doi: 10.4103/2230-8210.109667 PMCID: PMC3683194 PMID: 23776892 Thyroid ultrasound Vikas Chaudhary and Shahina Bano1

[8] - Thyroid Volume in Hypothyroidism due to Autoimmune Disease Follows a Unimodal Distribution: Evidence against Primary Thyroid Atrophy and Autoimmune Thyroiditis Being Distinct Diseases Allan Carlé Inge Bülow Pedersen Nils Knudsen Hans Perrild Lars Ovesen Torben Jørgensen Peter Laurberg The Journal of Clinical Endocrinology & Metabolism, Volume 94, Issue 3, 1 March 2009, Pages 833–839, https://doi.org/10.1210/jc.2008-1370 Published: 01 March 2009 Article history

ARTICLE TITLE: Aortic calcification and aneurysm in Moscow Lung Cancer Screening.

AUTHORS: Korkunova O. A.1, Suchilova M. M.1, Nikolaev A. E.2, Grishkov S.M.2., Gombolevskiy V. A., Bosin V. Yu.

INSTITUTIONS:

1. FSBEI FPE RMACPE MOH, Russia
2. Research and Practical Clinical Center of Diagnostics and Telemedicine Technologies, Department of Health Care of Moscow, Russia

THESIS:
Objective: assess the prevalence of thoracic aortic calcification and aneurysm in patients in lung cancer screening.
Materials and methods: the retrospective study included randomly selected results of ultra-low-dose computed tomography of 254 patients.
Results: quantitative analysis of aortic calcination by Agatston, Volume, Mass index, as well as qualitative and quantitative analysis of aortic aneurysm occurrence in lung cancer screening was performed.
Conclusion: it is necessary to pay attention to the presence of thoracic aorta calcification and aneurysm in lung cancer screening, as these changes are closely associated with a high risk of cardiovascular diseases leading to death.

KEYWORDS: Aortic calcification, Aortic aneurysm, Ultra-low-dose computed tomography.

CORRESPONDING AUTHOR: Korkunova O. A.

E-MAIL: oa.korkunova@gmail.com

FOR CITATIONS: Korkunova O. A., Suchilova M. M., Nikolayev A. E., Grishkov S. M., Gombolevskiy V. A., Bosin V. Yu. - Aortic calcification and aneurysm in Moscow Lung Cancer Screening // Radiology Study. - 2019. - T1., №1. - p. 16-25

Aortic calcification in Moscow Lung Cancer Screening.

Introduction

Incidental findings are often detected by low-dose computed tomography (LDCT), which is used in lung cancer screening. For example, the National Lung Cancer Screening Trial (NLST) shows a 20% reduction in lung cancer mortality and an overall 6.7% reduction in mortality [1]. LDCT iis an informative method of imaging of the chest, which has an important advantage as low doses compared to standard protocols of computed tomography. In 2017, the project "Moscow lung cancer screening" was launched in Moscow through the use of ultra-low-dose computed tomography (ultra-LDCT), aimed at selective screening of lung cancer in the outpatient link [2]. The project was organized by the Research and Practical Clinical Center of Diagnostics and Telemedicine Technologies, Department of Health Care of Moscow, Russia.

In the protocols of the project "Moscow lung cancer screening" the permissible dose of radiation should be less than 1 mSv (Figure 1), while the image quality allows to evaluate the findings at a reliable level, which is important in the assessment of additional pathological changes.

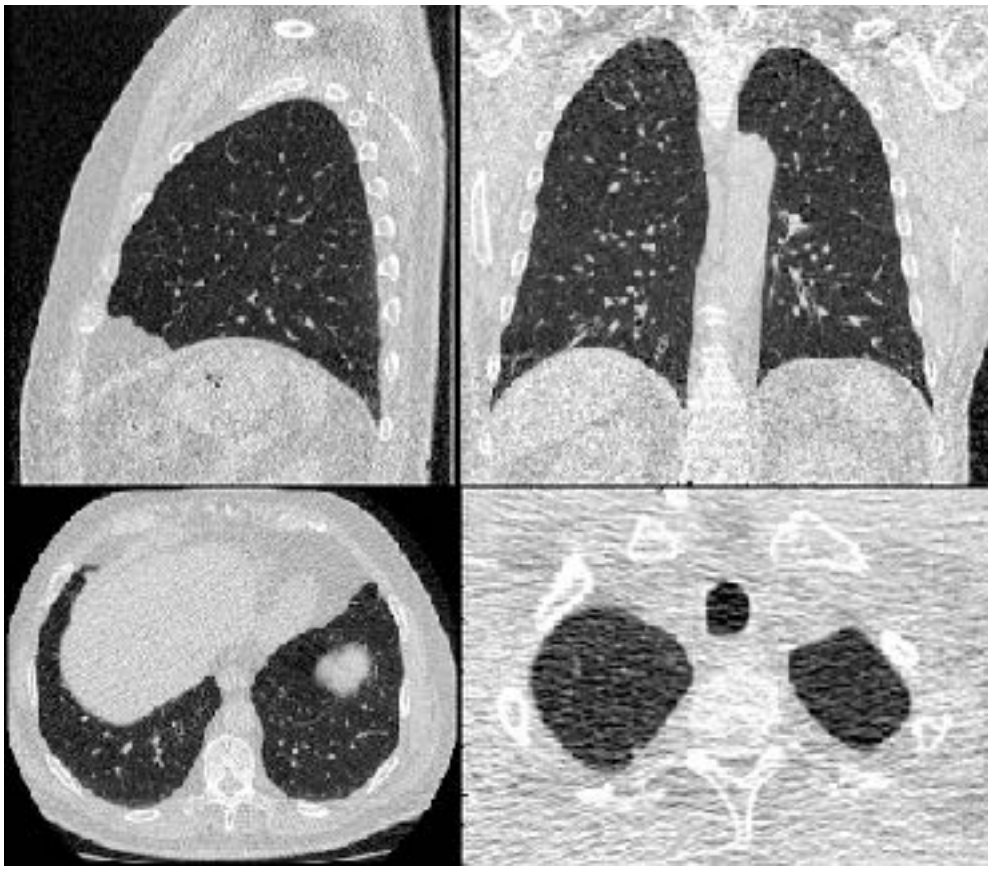

Figure 1. On these images demonstrate quality of LDCT for Moscow lung cancer screening. Please note on the quality in the upper and lower segments of the both lungs.

Ultra-LDCT images are suitable for recognition of obvious and potentially significant incidental findings. In lung cancer screening, early detection of accidental findings can reduce mortality in patients aged 55-75 years [3,4]. Ultra-LDCT screening promotes recognition of significant incidental findings, in particular, early detection of signs of chronic obstructive pulmonary disease and diseases of the cardiovascular system in the smoking population [5]. Established indicator of cardiovascular disease is coronary artery calcification, which is clearly correlated with an increase in the patient's age and the presence of Smoking in the history [6]. In NLST studies, 50% of deaths are associated with cardiovascular disease, as confirmed by observations in other cohorts [7].
Thoracic aorta calcification is associated with risk factors of atherosclerosis, although the pathogenesis and clinical manifestations remain not fully understood.
The native computer tomography (CT) distinguish the following patterns of aorta calcification (Figure 2): circumferential calcification in patients with post-radiation changes of the cardiovascular system, more confluent calcination in patients with inflammation of the walls of history and patchy calcification, which is typical of atherosclerosis [8].

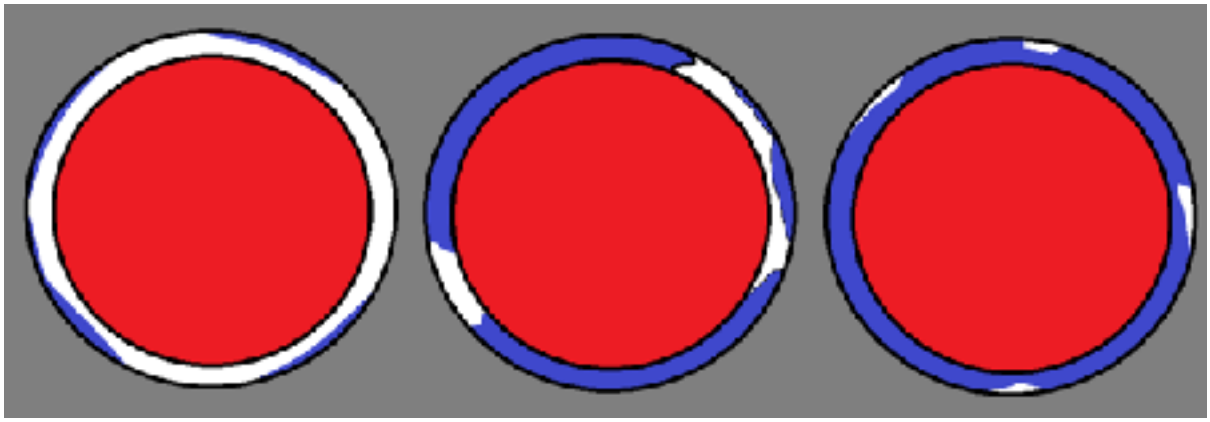

Figure 2. Patterns of aortic wall calcification. On noncontrast-enhanced computed tomography (CT) scans is possible to visualize these patterns of calcification: (right) circumferential calcification in a patient with radiation-associated cardiovascular disease, (middle) more confluent calcification in a patient with a remote history of aortitis and (left) patchy calcification typical of atherosclerosis.

In a single-center clinical study, which involved 970 patients who applied to the cardiology Department, presented the distribution of the thoracic aorta calcification by segments. Calcifications were most often visualized in the aortic arch and proximal part of the descending aorta, which are not usually included in the scanning field during coronary calcium screening. The data are presented in the study of Cream and co-authors [9], and the results are presented below in figure 3.

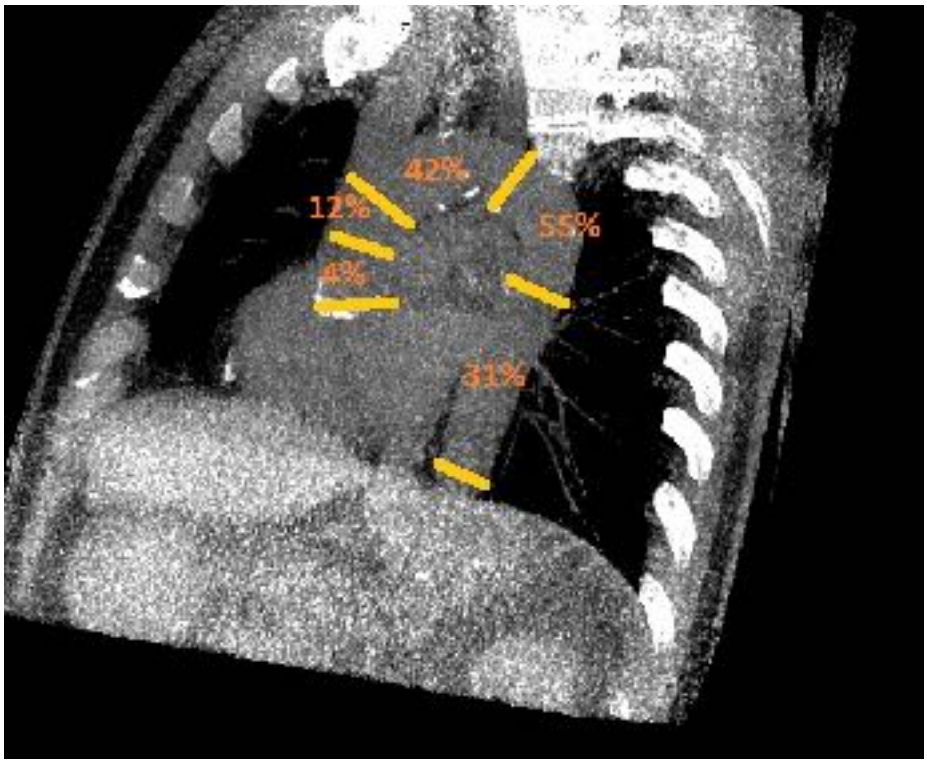

Figure 3. Distribution of thoracic aortic calcification.
In a single-center study of 970 patients referred to a cardiovascular prevention unit, percentages of patients with calcifications at different segments of the thoracic aorta are shown. Calcifications were most commonly visualized in the aortic arch and proximal descending aorta, which are segments not typically included in a CAC scan. Reproduced from data in Craiem et al. [50]

The aim of the study was to assess the prevalence of thoracic aortic calcification and aneurysm in patients of lung cancer screening.

Materials and Methods.

During the primary (baseline) screening round 5,310 ultra-LDCT were conducted in 10 medical organizations providing primary health care to the adult population of Moscow. The studies were carried out on the Toshiba Aquilion 64 computed tomographic scanner using specially developed ultra-low-dose protocols for different patient weight categories with radiation dose up to 1 mSv. 4,762 (89.7% from 5,310 studies,) were performed in individuals who met the criteria for inclusion in the risk group for lung cancer. A certain part of these patients was referred to oncologist, phthisiologist, therapist [10].
In the first part of the study, implying a qualitative assessment of aortic changes, included 254 (4.78%) ultra-LDCT, which were selected using a generator of random number. At the same time, the results of patients who were routed for additional examinations and consultations on the results of ultra-LDCT were not considered. The selected group included

the results of ultra-LDCT 142 (56.0%) men and 112 (44.0%) women; the average age was 61 years. The exact age distribution of the surveyed: 55-59 years – 25.2% (64), 60-64 years – 25.2% (64), 65-69 years – 24.8% (63), 70-74 years – 24.8% (63).
In the second part of the study, implying a quantitative assessment of aortic calcification, included 25 (0.471%) ultra-LDCT, which were selected using a random number generator. At the same time, the results of patients who were routed for additional examinations and consultations on the results of ultra-LDCT were not considered. The selected group included the results of ultra-LDCT of 10 (40.0%) men and 15 (60.0%) women in the age group of 70-74 years.
A retrospective review of the results (images and reports of chest ultra-LDCT performed within the framework of the project "Moscow screening of lung cancer" in 2017) for a preliminary assessment of the prevalence of thoracic aortic calcification was carried out. The review was carried out by two independent experts with more than 7 years of experience in thoracic radiology, followed by a panel discussion.
Medical data has been depersonalized in accordance with applicable personal data protection legislation. The image analysis in DICOM 3.0 standard was carried out using the software "AGFA Agility Enterprise 8.0" and "OsiriX MD (V. 5.5.1 64-bit)". Quantitative data were obtained and analyzed. Quantitative analysis of aortic calcination by The Agatston, Volume, Mass index was carried out using the standard scanning technique during screening using ultra-LDCT with a thickness of slice in 1 mm. Aortic calcification was evaluated semi-automatically, as shown in the image below (Figure 4). The protocols of the description searched for all pathological findings related to the calcification of the thoracic aorta.

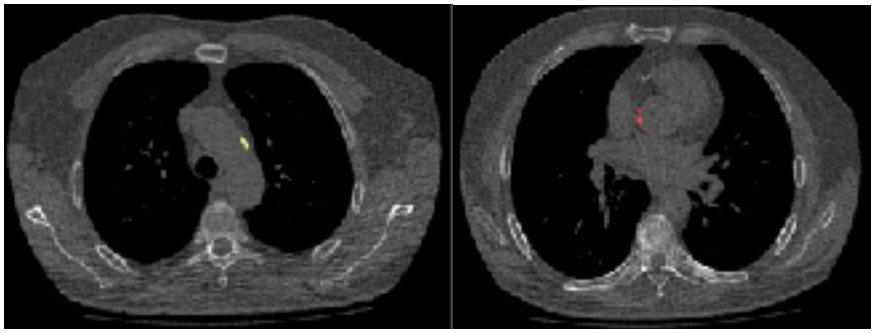

Figure 4.
On these images it demonstrates semiautomatic segmentation of thoracic aorta calcification with Osirix software.

Results.
The localization of incidental findings was as follows: lungs and bronchi – 68.3% (174) of cases, pleura – 2.75% (7), cardiovascular system – 75.4% (192), mediastinum – 2.75% (7), some organs of the abdominal cavity and retroperitoneal space – 4.2% (10), endocrine system organs – 2.7% (7), mammary glands – 0.8% of cases.

A total of 58.4% (148/254) of random findings were not described in the initial reports of ultra-LDCT.

In the primary description of ultra-LDCT, radiologists most often did not indicate changes in the adrenal glands in the reports (in 3 cases, all 100.0% are not indicated), expansion of the pulmonary trunk (19 – 100.0%), expansion of the ascending and descending aorta (159 -82.3%), and the presence of coronary calcium (64 -33.0%).
All incidental findings of the cardiovascular system revealed at 76.4% (169/221) cases. In the primary reports of ultra-LDCT 67,0% (113) were specified, thus any recommendations (for example, consultation of the cardiologist) were not given. The structure of the most frequent incidental findings of the cardiovascular system is shown in figure 1.
In most cases (64,5%; 124/169) incidental finding was calcification of the coronary arteries, but despite this, the aneurysm and calcification of the aorta together comprise almost a quarter (26,7%; 45/169).

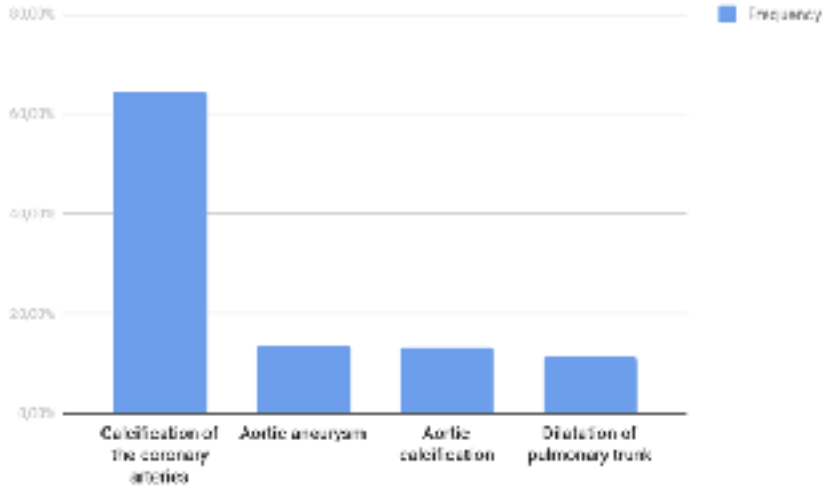

Graph №1. The structure of the most frequent random findings of the cardiovascular system in Moscow Lung Cancer Screening.

In the reports of ultra-LDCT, radiologists did not indicate the presence of coronary calcium in 33%, aortic calcification in 25%, ascending and descending aorta dilation in 82.3% of cases, and pulmonary trunk dilation in 100%. Thus, in those opinions, which marked the presence of the above changes of the cardiovascular system, all reports were absent recommendation part. In CT images, coronary calcium was found in 64.5% of cases, ascending and descending aorta dilation in 13.7% and 11.4% of cases, respectively, and pulmonary trunk dilation in 11.4% of cases. The average morphometry of the ascending and descending aorta and pulmonary trunk was 35.3+/-4.5 cm, 26.5+/-3.5 cm, 25.3+/-3.8 cm, respectively (see table 1).
Table 1. Qualitative and quantitative analysis of aortic aneurysm occurrence.

Value	N	Arithmetic mean	% of normal	Average square deviation	Average error	Cs
The diameter of the ascending aorta	254	35,33	85.4%	4,51	2,22	0,063
The diameter of the descending aorta	254	26,51	88.4%	3,50	1,663	0,063

Retrospectively, 25 patients were evaluated for aortic calcification by Agatston, Volume, Mass, the corresponding results are presented in table 2 below.

Table 2. Assessment of aortic calcification by Agatston, Volume, Mass.

	Total calcification of the aorta (Agatston)	Total aortic calcification (Volume)	Total aortic calcification (Mass)
N	25	25	25
Arithmetic mean	7000,40	2277,64	4095,80
Average square deviation	7833,33	2426,15	4717,88
Maximal value	24953	7897	13917
Minimal value	342	107	147

Discussion.

Based on the results of the analysis of the data obtained during the NLST screening program, the clinical significance of coronary artery calcification in lung cancer screening with LDCT was proved [11]. However, as and some other incidental findings [2].

Evaluation of coronary calcium contributes to earlier treatment administration, while most of the examined persons are already candidates for therapy only on the basis of two indicators (age and time of smoking) [11].

One of the frequent findings was an aortic aneurysm (more than 4.1 cm in diameter), rarely indicated in the primary reporting. In such a situation, it is justified to refer patients for re-examination after 6 months due to the circumstances specified below.

Surgical intervention in aortic aneurysm is indicated [12]:

- with a growth rate of more than 0.5 cm per year;
- the initial diameter of the thoracic aorta is more than 5.5 cm (in the initial study);

- the initial diameter of the thoracic aorta is more than 4.4-5.0 cm against the background of systemic connective tissue disease or in the presence of symptoms.

Quantify the calcification of the aorta is not yet developed scale with the recommendation part (by analogy with the conventional scale of Agatston), which is a promising topic for future research. The intensive development of automatic segmentation and artificial intelligence should facilitate the approach to solving this problem, and it will allow to obtain more information about the patient in lung cancer screening.
Early detection of clinically significant changes in the cardiovascular system, such as thoracic aorta aneurysm and calcification, is possible with ultra-LDCT in lung cancer screening, which will help to reduce mortality rates in general population.

Conclusion

Upon detection of changes in the cardiovascular system with ultra-HDCT in lung cancer screening, it is necessary to carefully evaluate these changes of the aorta such as its diameter and the presence of calcification. In the reporting is important to note the presence of the thoracic aorta calcification, as well as be sure to send the patient to the consultation of a cardiologist, because these changes are associated with a high risk of cardiovascular diseases that lead to death.

Disclosures

The authors declare that there is no conflict of interest

References:

1. National Lung Screening Trial Research Team, Aberle DR, Adams AM, et al: Reduced Lung-Cancer Mortality with Low-Dose Computed Tomographic Screening. N Engl J Med 365:395-409, 2011

2. Gombolevskiy V.A., Kharlamov K.A., Pyatnitskiy I.A., Kim S.Yu., Morozov S.P. Shablony protokolov opisaniy issledovaniy po spetsialnosti rentgenologiya. Kompyuternaya tomografiya. [Protocol templates for description of X-ray examinations. Computed tomography]. GBUZ Goroda Moskvy Nauchno-Prakticheskiy Tsentr Meditsinskoy Radiologii Departamenta Zdravookhraneniya Goroda Moskvy Publ.

3. National Center for Chronic Disease Prevention and Health Promotion (US) Office on Smoking and Health: The Health Consequences of Smoking—50 Years of Progress: A Report of the Surgeon General [Internet]. Atlanta (GA): Centers for Disease Control and Prevention (US), 2014. [cited 2017 Aug 24]. (Reports of the Surgeon General). Available from: http://www.ncbi.nlm.nih.gov/books/NBK179276/

4. Final Update Summary: Lung Cancer: Screening - US Preventive Services Task Force [Internet]. [cited 2017 Aug 22]. Available from: https://www.uspreventiveservicestaskforce.org/Page/Document/UpdateSummaryFi nal/lung-cancer-screening.

5. Incidental Findings on Lung Cancer Screening: Significance and Management Emily B. Tsai, MD, Caroline Chiles, MD, Brett W. Carter, MD, Myrna C.B. Godoy, MD, PhD, Girish S. Shroff, MD, Reginald F. Munden, MD, DMD, MBA, Mylene T. Truong, MD, and Carol C. Wu, MD

6. Oei HH, Vliegenthart R, Hofman A, et al. Risk factors for coronary calcification in older subjects. The Rotterdam Coronary Calcification Study. Eur Heart J 2004;25:48–55.

7. Chiles C, Duan F, Gladish GW, et al. Association of coronary artery calcification and mortality in the national lung screening trial: a comparison of three scoring methods. Radiology 2015;276:82–90.

8. JACC Cardiovasc Imaging. 2018 Jul;11(7):1012-1026. doi: 10.1016/j.jcmg.2018.03.023. Thoracic Aortic Calcification: Diagnostic, Prognostic, and Management Considerations. Desai MY1, Cremer PC2, Schoenhagen P3.

9. Craiem D, Chironi G, Casciaro ME, Graf S, Simon A. Calcifications of the thoracic aorta on extended non-contrast-enhanced cardiac CT. PLoS One 2014;9:e109584.

10. Gombolevskiy V.A., Barchuk A.A., Laypan A.Sh., Vetsheva N.N. et al. Organization and efficiency of screening for malignant lung tumors by low-dose computed tomography. Radiologiya. Praktika. 2018, no. 1 (67), pp. 28-36. (In Russ.)

11. Chiles C., Duan F., Gladish G. W. et al. Association of coronary artery calcification and mortality in the National Lung Screening Trial: a comparison of three scoring methods // Radiology. – 2015. – Vol. 276. – P. 82-90.

12. National Center for Chronic Disease Prevention and Health Promotion (US) Office on Smoking and Health. The Health Consequences of Smoking – 50 Years of Progress: A Report of the Surgeon General. Atlanta (GA), Centers for Disease Control and Prevention (US), 2014. Available from: http://www.ncbi.nlm.nih.gov/books/NBK179276/

ARTICLE TITLE: **CT-density Atlas of abdominal structures on different voltages.**

AUTHORS: Nikolaev A.E., Gonchar A.P., Petraikin A.V., Chernina V.U., Semenov D.S., Akhmad E.S.
INSTITUTIONS:
1. Research and Practical Clinical Center of Diagnostics and Telemedicine Technologies, Department of Health Care of Moscow, Russia

THESIS:
This paper presents the results of measuring the X-ray density (HU) of the structures of the patient's abdominal cavity at various voltages (40–200 kVp). The patient study was performed in the dual-energy mode with subsequent imaging at intermediate energies. The mean values of HU, standard deviation, maximum and minimum values for the following areas are presented: liver, spleen, kidney, adrenal glands, aorta, vertebral body, muscle, subcutaneous fat, visceral fat. The tables in this article can be used in practice for a more accurate interpretation of the densities of anatomical structures, which are measured on images obtained at different voltages.

KEYWORDS: computed tomography, X-ray density, different voltages on CT, abdominal structures

CORRESPONDING AUTHOR:
Nikolaev Alexander
E-MAIL: a.e.nikolaev@yandex.ru

FOR CITATIONS: Nikolaev A.E., Gonchar A.P., Petraikin A.V., Chernina V.U., Semenov D.S., Akhmad E.S. - CT-density Atlas of abdominal structures on different voltages. // Radiology Study. - 2019. - T1., №1. - p. 26-43

Introduction

Since the creation of computed tomography (CT) in the 1970s, its use has grown rapidly due to its important role in clinical diagnosis and widespread accessibility (1). Although CT accounts for only 15% of all medical imaging procedures, it goes to make up at least half of the radiation exposure to medical imaging (2, 3), and CT is the largest source of radiation in the developed countries (4). This problem led to the optimization of the low dose CT-imaging protocols as possible without compromising the quality of the diagnostic image (5).

On the other hand, we can observe that changes in scanning protocols contribute to changes in the density parameters of organs and tissues visualized on CT.

This fact was clearly demonstrated in the article by Dong Joo Hee and co-authors (6).

In this study, the density difference was shown to be the same for most structures, with the exception of air, where the density is very low and, therefore, noise affects the image more significantly than the cross-section differences from various photon energies (6).

Low-dose computed tomography is a diagnostic method with low radiation, for this reason it is used everywhere in the imaging, especially in the screening of lung cancer, pediatric imaging, cardiac imaging with iterative reconstruction, radiation therapy, hybrid nuclear imaging. Inasmuch as a low-dose computed tomography is used in many diagnostic tasks, we assume that radiologists experience problems with reliable density measurement in their practice.

Recently, a tomography with a new spectral detector has appeared as an original solution, it retrospectively generates several layers of spectral data for a single scan with a low dose of radiation. Fully adaptable to the current workflow, this specially designed solution provides high diagnostic quality (7). The reliability of clinical results increases and the correct diagnosis is possible already in the first scan.

We didn't find any information in the medical literature about changes in the density of particular anatomical structures depending on the variation of the voltage during scanning, which radiologists can use easily in their practice.

For these reasons, we decided to develop an Atlas of computed tomograms obtained at different voltages during scanning.

Below is a table of the researched structures densities on the standard voltage (120 kVp) and references:

Substance	Density (HU)	Reference
Air	–1000	
Water	0	
Fat	–120 to –90	Herbert Lepor (2000). Prostatic Diseases. W.B. Saunders Company. ISBN 9780721674162.

Soft Tissue, Contrast			
Blood	Unclotted	+13 to +50	Robert Fosbinder, Denise Orth (2011). Essentials of Radiologic Science. Lippincott Williams & Wilkins. ISBN 9780781775540. page 20.17 in: F W Wright (2001). Radiology of the Chest and Related Conditions. CRC Press. ISBN 9780415281416.
	clotted	+50 to +75	Dr. Avital Fast, Dorith Goldsher (2006). Navigating the Adult Spine: Bridging Clinical Practice and Neuroradiology. Demos Medical Publishing. ISBN 9781934559741.
	Subdural hematoma, first hours	+75 to +100	Rao, Murali Gundu (2016). "Dating of Early Subdural Haematoma: A Correlative Clinico-Radiological Study". Journal of Clinical and Diagnostic Research. 10 (4): HC01–5. doi:10.7860/JCDR/2016/17207.7644. ISSN 2249-782X. PMC 4866129 Freely accessible. PMID 27190831.
	Subdural hematoma, after 3 days	+65 to +85	Rao, Murali Gundu (2016). "Dating of Early Subdural Haematoma: A Correlative Clinico-Radiological Study". Journal of Clinical and Diagnostic Research. 10 (4): HC01–5. doi:10.7860/JCDR/2016/17207.7644. ISSN 2249-782X. PMC 4866129 Freely accessible. PMID 27190831.
	Subdural hematoma, after 10-14 days	+35 to +40	Dr Rohit Sharma and A.Prof Frank Gaillard. "Subdural haemorrhage". Radiopaedia. Retrieved 2018-08-14.
	Chyle	–30	*Luca Saba, Jasjit S. Suri (2013). Multi-Detector CT Imaging: Principles, Head, Neck, and Vascular Systems, Volume 1. CRC Press. ISBN 9781439893845.*
	Urine	-5 to +15	*Herbert Lepor (2000). Prostatic Diseases. W.B. Saunders Company. ISBN 9780721674162.*
	Bile	-5 to +15	Herbert Lepor (2000). Prostatic Diseases. W.B. Saunders Company. ISBN 9780721674162.
	Abscess	+20 to +40	Sasaki, Toru; Miyata, Rie; Hatai, Yoshiho; Makita, Kohzoh; Tsunoda, Koichi (2014). "Hounsfield unit values of retropharyngeal abscess-like lesions seen in Kawasaki disease". Acta Oto-Laryngologica. 134 (4): 437–440. doi:10.3109/00016489.2013.878475. ISSN 0001-6489. PMID 24512428.

Other fluids	Mucus	0 - 130 ("high attenuating" at over 70 HU)	K SAGGAR, A AHLUWALIA, P SANDHU, V KALIA (2006). "Mucocoele Of The Appendix"(PDF). Ind J Radiol Imag. 16 (2).
Parenchyma	Lung	-700 to –600	Ella A. Kazerooni, Barry H. Gross (2004). Cardiopulmonary Imaging. 4. Lippincott Williams & Wilkins. ISBN 9780781736558.
	Kidney	+20 to +45	Herbert Lepor (2000). Prostatic Diseases. W.B. Saunders Company. ISBN 9780721674162.
	Liver	60 ± 6	Erwin Kuntz, Hans-Dieter Kuntz (2006). Hepatology, Principles and Practice: History, Morphology, Biochemistry, Diagnostics, Clinic, Therapy. Springer Science & Business Media. ISBN 9783540289777.
	Lymph nodes	+10 to +20	G. Maatman (2012). High-Resolution Computed Tomography of the Paranasal Sinuses and Pharynx and Related Regions: Impact of CT identification on diagnosis and patient management. Volume 12 of Series in Radiology. Springer Science & Business Media. ISBN 9789400942776.
	Muscle	+35 to +55	Herbert Lepor (2000). Prostatic Diseases. W.B. Saunders Company. ISBN 9780721674162.
	Thymus	+20 to +40 in children +20 to +120 in adolescents	Jean-Claude Givel, Marco Merlini, David B. Clarke, Michael Dusmet (2012). Surgery of the Thymus: Pathology, Associated Disorders and Surgical Technique. Springer Science & Business Media. ISBN 9783642710766.
Gallstone	Cholesterol stone	+30 to +100	Rambow A, Staritz M, Wosiewitz U, Mildenburger P, Thelen M, Meyer zum Büschenfelde KH (1990). "Analysis of radiolucent gallstones by computed tomography for in vivo estimation of stone components". Eur J Clin Invest. 20 (4): 475–8. PMID 2121509.
	Bilirubin stone	+90 to +120	Mildenburger P, Thelen M, Meyer zum Büschenfelde KH (1990). "Analysis of radiolucent gallstones by computed tomography for in vivo estimation of stone components". Eur J Clin Invest. 20 (4): 475–8. PMID 2121509.

Material and methods

Multienergetic computed tomograms were used to evaluate abdominal structures. Originally, these unenhanced helical computed tomograms were performed on the occasion of urolithiasis.

The following anatomical structures were selected for evaluation:

- Liver
- Spleen
- Kidney
- Adrenal glands
- Aorta
- Vertebral body
- Muscle
- Subcutaneous fat
- Visceral fat

The same ROI area equal to 1.2 cm2 was chosen to evaluate the above structures, except for the adrenal glands. An area of 0.3 cm2 was chosen for the adrenal glands.

The density of anatomical structures was measured on two different slices, on different voltages, but in the same localization of each anatomical structure, which is represented on the two images below.

The following voltage parameters, witch are most commonly used in practice, were selected for our Atlas, such as 40, 60, 70, 80, 90, 100, 110, 120, 135, 140, 160, 180, 200 kVp.

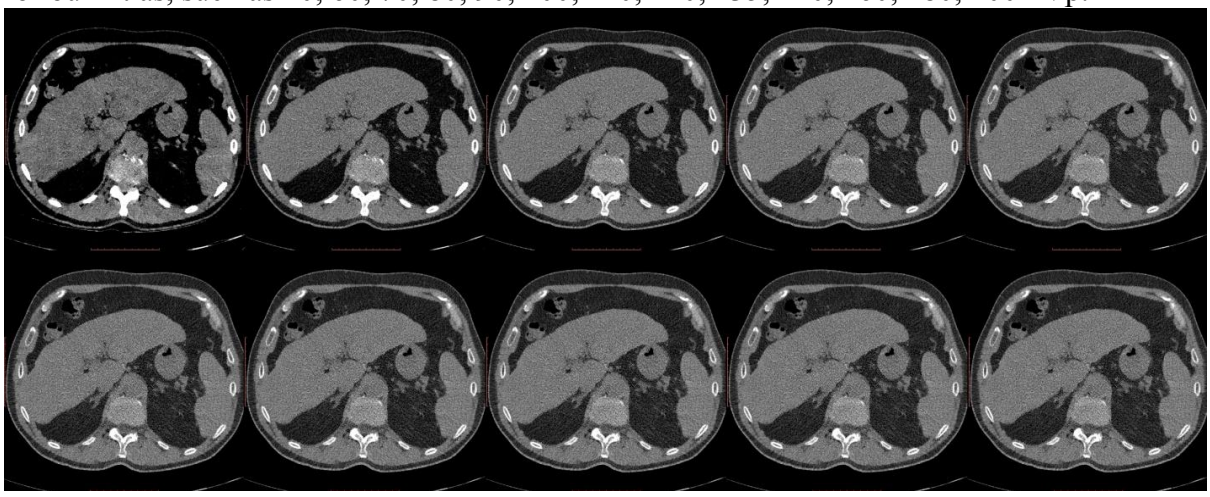

Figure №1 The images are presented on the same slice, but on different voltages. The following anatomical structures were evaluated in these images: liver, spleen, adrenal glands, muscles, aorta.

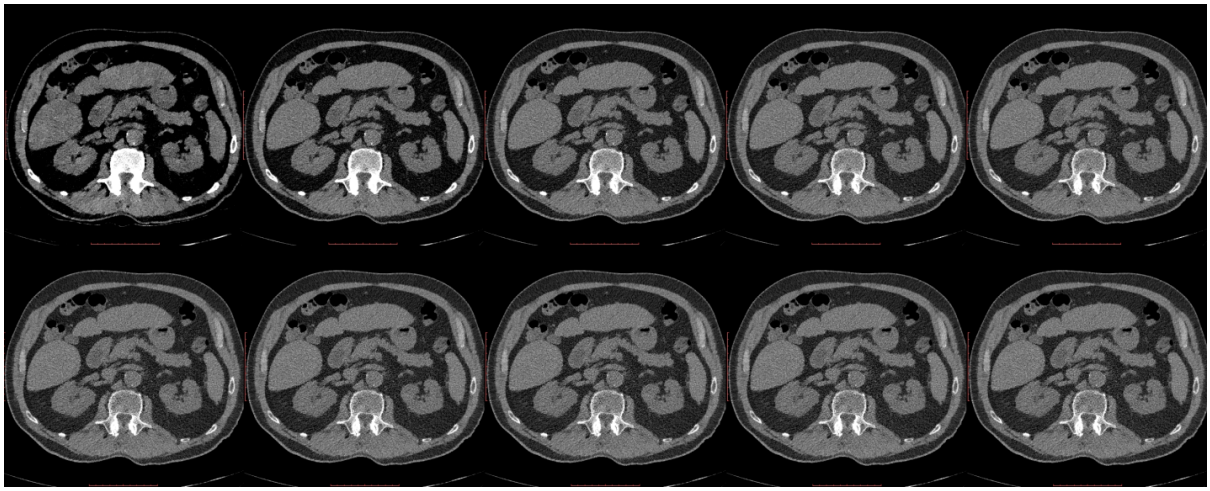

Figure №2
The images are presented on the same slice but on different voltages. The following anatomical structures were evaluated in these images: kidneys, subcutaneous and visceral fat, vertebral body.

Results

The results of density measurements at different voltages are presented below for each anatomical structure. The results are presented in a table showing the mean values, standard deviation, maximum and minimum values. A diagram for each anatomical structure, that shows the trend of density variations depending on the changes in the voltage, is also provided.

Voltage (kVp)	Density (HU)	SD	Min	Max
40	36,2	28,9	-70	109
60	40,6	28,7	-61	120
70	41,1	28,6	-59	121
80	41,7	28,3	-58	124
90	42,2	27,9	-57	124
100	42,8	27,7	-56	125
110	42,6	27,7	-56	125
120	42,3	27,7	-56	126
135	42,4	27,7	-56	126
140	42,6	27,9	-56	126
160	43,4	27,1	-55	117
180	43,7	27,9	-55	127
200	43	27,2	-55	117
Mean value density (HU)		**Standard deviation**	**Maximal density (HU)**	**Minimal density (HU)**
41,87		2,06	43,7	36,2

Table №1 summaries the results of liver densities variability.

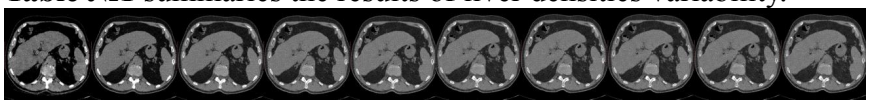

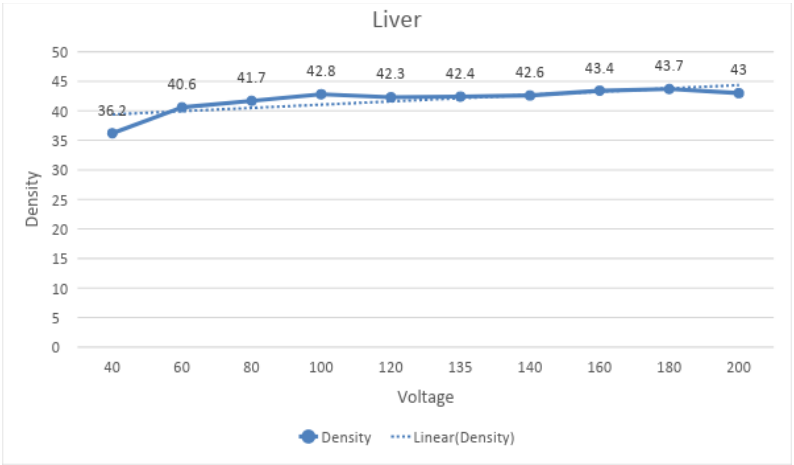

Diagram №1 demonstrates the change in liver density depending on the voltage.

Voltage (kVp)	Density (HU)	SD	Min	Max
40	44,2	30,9	-37	131
60	45,9	29,3	-39	129
70	45,9	29,4	-39	129
80	45,9	29,6	-39	129
90	45,5	29,2	-39	129
100	45,3	28,7	-39	128
110	45,6	28,8	-39	128
120	45,9	28,9	-40	128
135	46	29,1	-40	128
140	46,3	29,5	-40	128
160	45,8	28,5	-40	128
180	44,9	29,2	-40	128
200	45,9	28,6	-40	128
Mean value density (HU)		**Standard deviation**	**Maximal density (HU)**	**Minimal density (HU)**
45,61		0,59	46,3	44,2

Table №2 summaries the results of muscle densities variability.

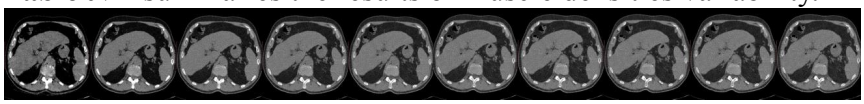

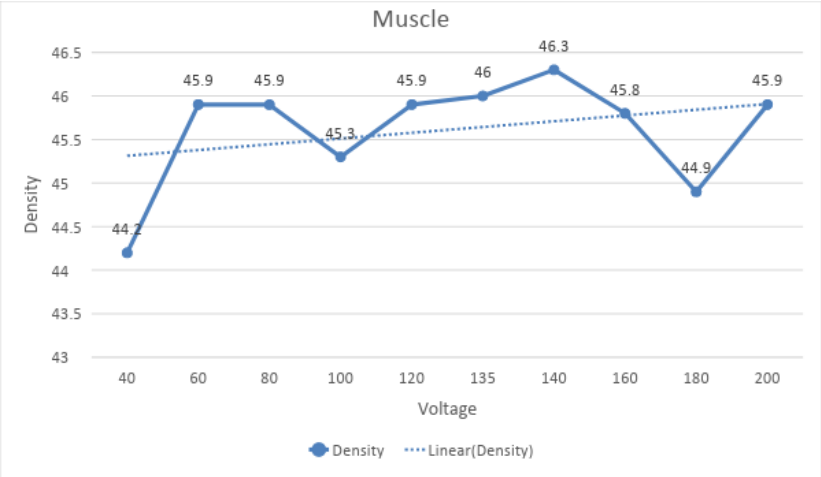

Diagram №2 demonstrates the variation of muscle density depending on the voltage.

Voltage (kVp)	Density	SD	Min	Max
40	-179,8	19,2	-242	-128
60	-119,4	18,4	-179	-71
70	-107,2	18,4	-167	-62
80	-97,8	18,4	-158	-51
90	-93,4	18,3	-154	-47
100	-88,6	18,3	-149	-42
110	-85,2	18,1	-146	-39
120	-84,1	18	-145	-37
135	-82,4	18,4	-145	-36
140	-81,9	18,58	-142	-35
160	-80,5	18,3	-141	-34
180	-80	17,84	-140	-33
200	-79,8	17,6	-139	-32
Mean value density (HU)		**Standard deviation**	**Maximal density (HU)**	**Minimal density (HU)**
-97,43		29,81	-79,8	-179,8

Table №3 summaries the results of subcutaneous fat densities variability.

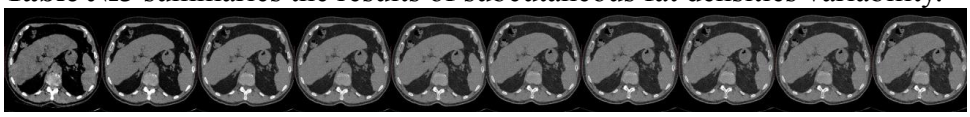

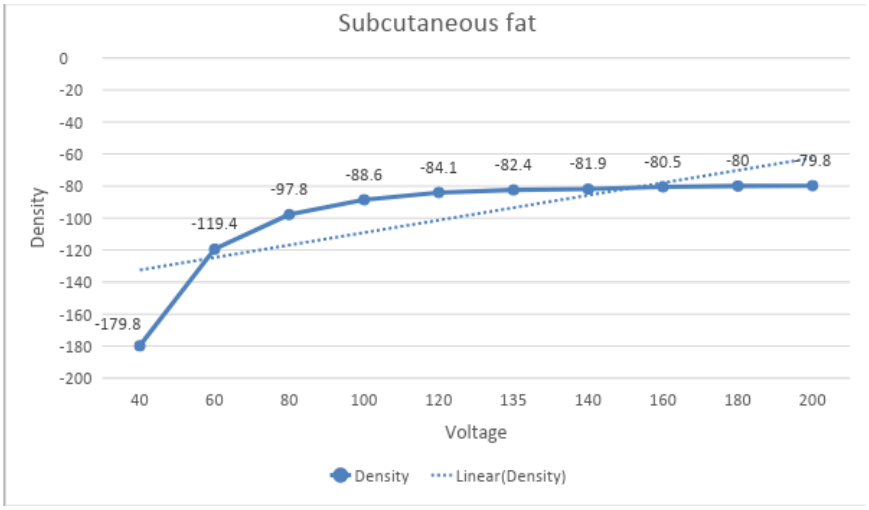

Diagram №3 demonstrates the variation of subcutaneous fat density depending on the voltage.

Voltage (kVp)	Density	SD	Min	Max
40	18,1	30,7	-66	92
60	27,3	29,6	-55	103
70	29,1	29,4	-53	104
80	30,8	29,2	-52	106
90	31,2	29,5	-51	107
100	31,7	29,8	-50	108
110	31,8	29,6	-50	108
120	31,9	29,5	-49	109
135	32,3	29,4	-49	109
140	32,8	29	-49	110
160	32,9	29,8	-48	112
180	32,7	28,34	-48	113
200	33,6	29,2	-48	111
Mean value density (HU)		**Standard deviation**	**Maximal density (HU)**	**Minimal density (HU)**
30,41		4,43	33,6	18,1

Table №4 summaries the results of right kidney densities variability.

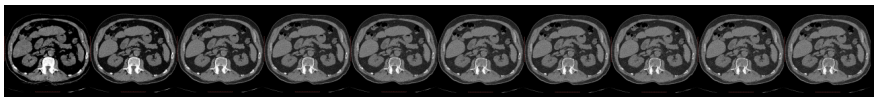

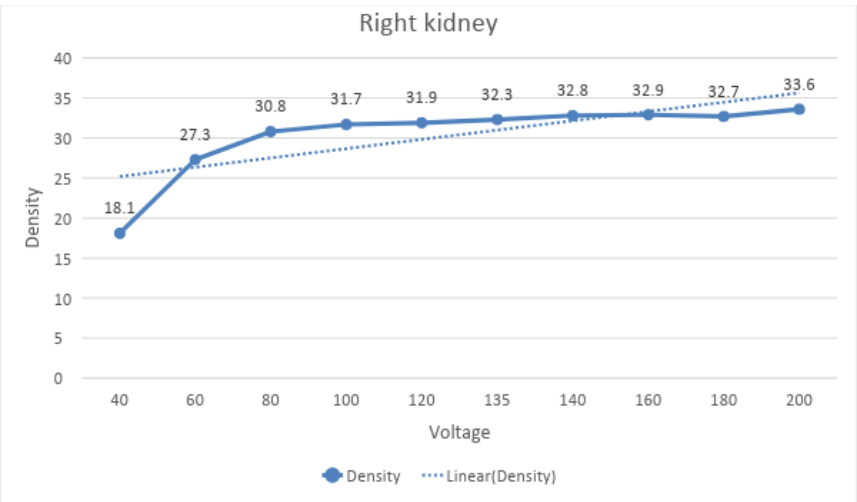

Diagram №4 demonstrates the variation of right kidney density depending on the voltage.

Voltage (kVp)	Density (HU)	SD	Min	Max
40	24,9	31,5	-73	109
60	30,1	29,4	-58	116
70	31,1	28,9	-55	114
80	31,8	28,3	-53	112
90	31,8	27,4	-52	113
100	31,9	26,7	-51	113
110	32,2	27,1	-51	113
120	32,4	26,9	-50	114
135	33,1	27,2	-50	114
140	33,7	27,5	-49	114
160	32,5	27,1	-49	114
180	33,4	27,7	-48	114
200	33,2	27,1	-48	114
Mean value density (HU)		**Standard deviation**	**Maximal density (HU)**	**Minimal density (HU)**
31,7		2,47	33,7	24,9

Table №5 summaries the results of left kidney densities variability.

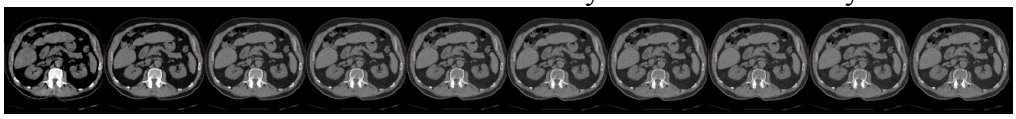

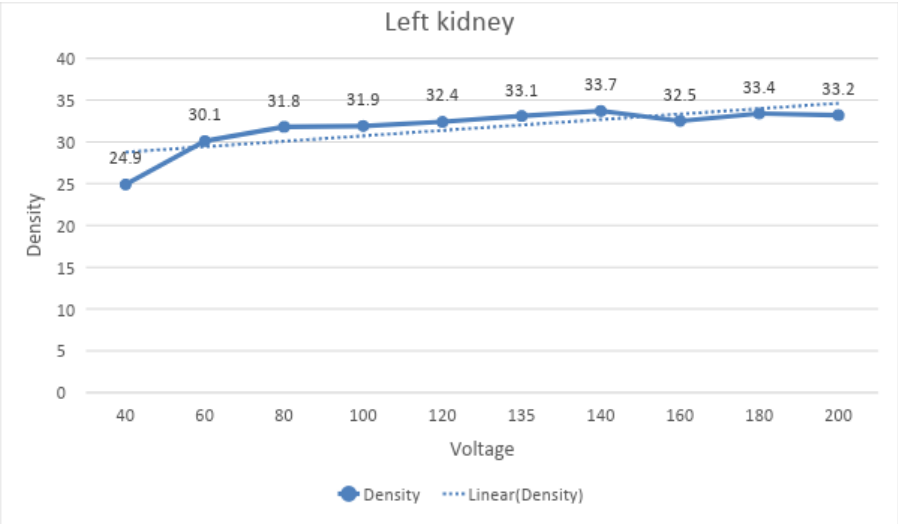

Diagram №5 demonstrates the variation of left kidney density depending on the voltage.

Voltage (kVp)	Density (HU)	SD	Min	Max
40	240,9	47,5	109	382
60	132,3	40,8	21	245
70	110,1	39,2	9	221
80	88,6	37,6	-22	196
90	79,8	37,5	-31	184
100	71,1	37,5	-43	175
110	65,9	37,8	-48	171
120	60,7	37,9	-49	165
135	58,1	37,5	-50	161
140	56	37,1	-55	159
160	54,3	37,2	-57	155
180	52,6	35,5	-46	153
200	50,1	37,4	-51	152
Mean value density (HU)		**Standard deviation**	**Maximal density (HU)**	**Minimal density (HU)**
86,47		56,6	240,9	50,1

Table №6 summaries the results of vertebral body densities variability.

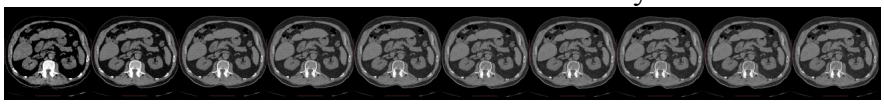

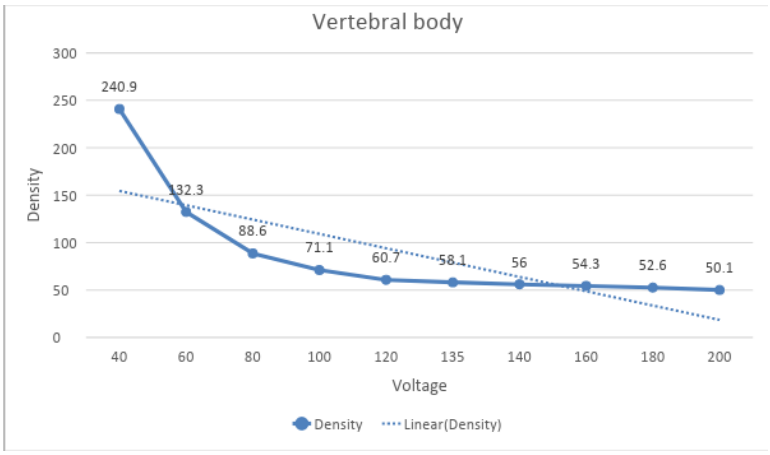

Diagram №6 demonstrates the variation of vertebral body density depending on the voltage.

Voltage (kVp)	Density (HU)	SD	Min	Max
40	45,9	32,8	-33	127
60	48	28,6	-47	114
70	49,6	27,6	-38	116
80	51	26,9	-10	117
90	50,8	26,8	-25	118
100	50,7	26,7	-38	119
110	50,8	26,7	-37	119
120	50,9	26,8	-37	120
135	51,2	26,5	-20	120
140	52	26,3	-8	120
160	51,9	26,3	-8	120
180	51,8	26,1	-7	121
200	52,2	25,9	-7	121

Mean value density (HU)	Standard deviation	Maximal density (HU)	Minimal density (HU)
50,56	1,92	52,2	45,9

Table №7 summaries the results of spleen densities variability.

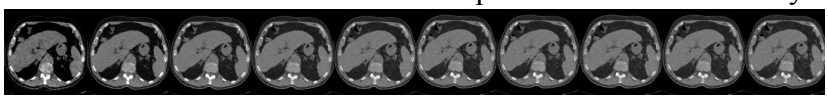

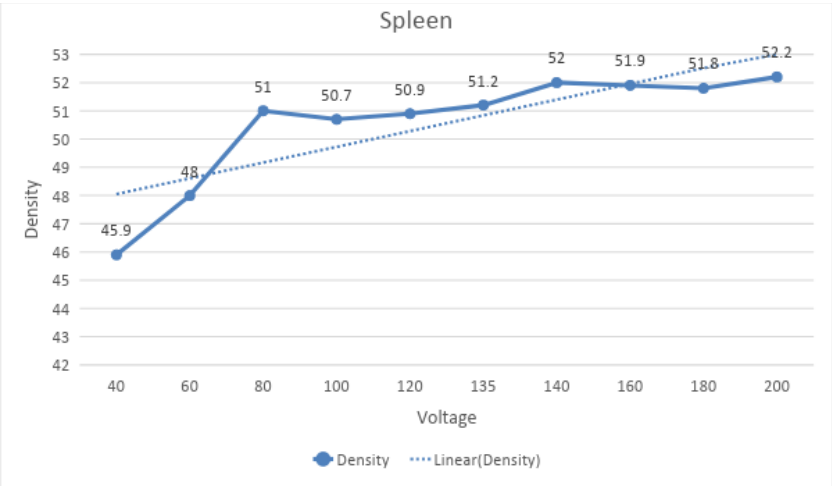

Diagram №7 demonstrates the variation of spleen density depending on the voltage.

Voltage (kVp)	Density	SD	Min	Max
40	-183,6	24,24	-244	-117
60	-123,1	22,9	-181	-59
70	-114,1	22,8	-172	-46
80	-101,9	22,7	-166	-38
90	-96,3	22,4	-160	-34
100	-92,6	22,1	-157	-29
110	-91,1	22,1	-153	-26
120	-87,7	22,6	-151	-24
135	-85,8	22,4	-148	-23
140	-84,7	22	-141	-22
160	-83,8	22,2	-146	-21
180	-82	22,3	-139	-20
200	-82	21,9	-138	-19
Mean value density (HU)		**Standard deviation**	**Maximal density (HU)**	**Minimal density (HU)**
-100,72		30,1	-82	-183,6

Table №8 summaries the results of visceral fat densities variability.

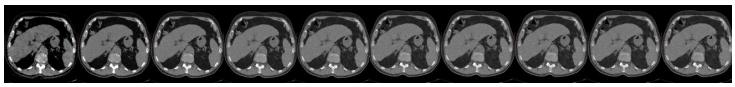

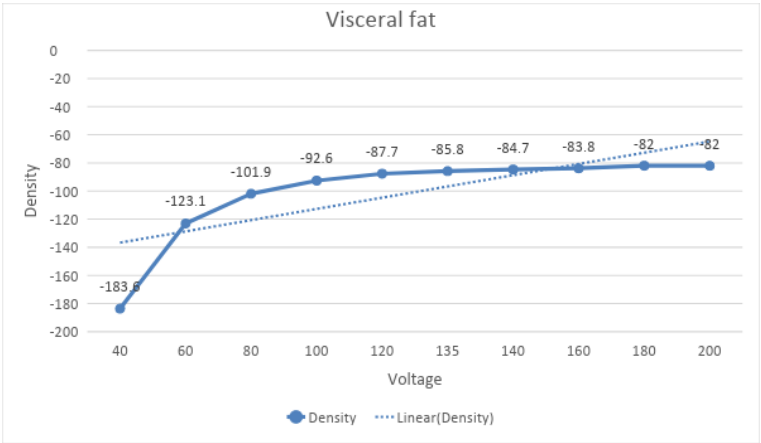

Diagram №8 demonstrates the variation of visceral fat density depending on the voltage.

Voltage (kVp)	Density	SD	Min	Max
40	40,9	39,5	-78	144
60	40,5	38,9	-71	132
70	40,2	38,2	-70	130
80	39,7	37,6	-69	126
90	39,2	37,6	-69	128
100	38,7	37,6	-68	129
110	39,2	37,4	-68	128
120	39,5	37,2	-68	127
135	39,4	37,2	-68	127
140	39,1	37,2	-67	130
160	38,5	37,5	-67	130
180	38,8	37,2	-67	130
200	38,1	37,1	-67	130
Mean value density (HU)		**Standard deviation**	**Maximal density (HU)**	**Minimal density (HU)**
39,32		0,83	40,9	38,1

Table №9 summaries the results of aorta densities variability.

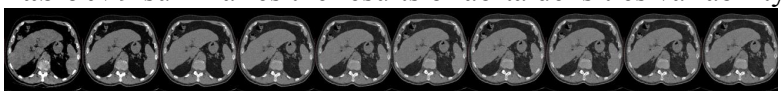

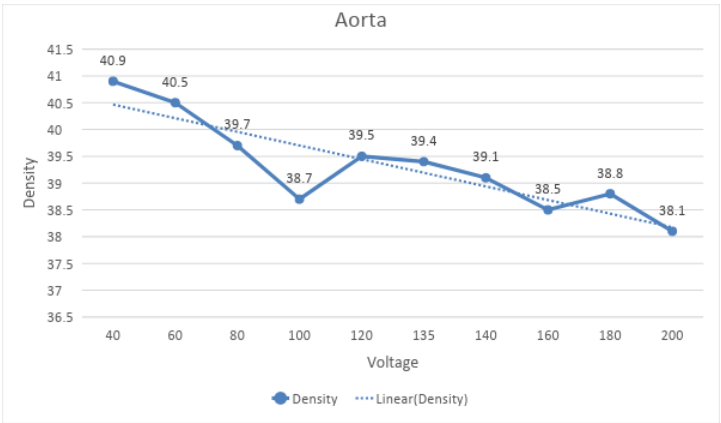

Diagram №9 demonstrates the variation of aorta density depending on the voltage.

Voltage (kVp)	Density	SD	Min	Max
40	21,5	36	-70	100
60	15,3	33,3	-61	84
70	14,6	32,9	-59	82
80	14	32,6	-58	80
90	12,4	31,4	-57	75
100	10,2	27,2	-56	72
110	10,9	28,9	-56	75
120	11,7	31,3	-56	75
135	11,5	31,2	-56	75
140	11	31,1	-55	75
160	12,9	28,2	-55	74
180	11,6	29,3	-55	74
200	11,6	28,1	-55	74
Mean value density (HU)		**Standard deviation**	**Maximal density (HU)**	**Minimal density (HU)**
13,13		3,13	21,5	10,2

Table №10 summaries the results of right adrenal gland densities variability.

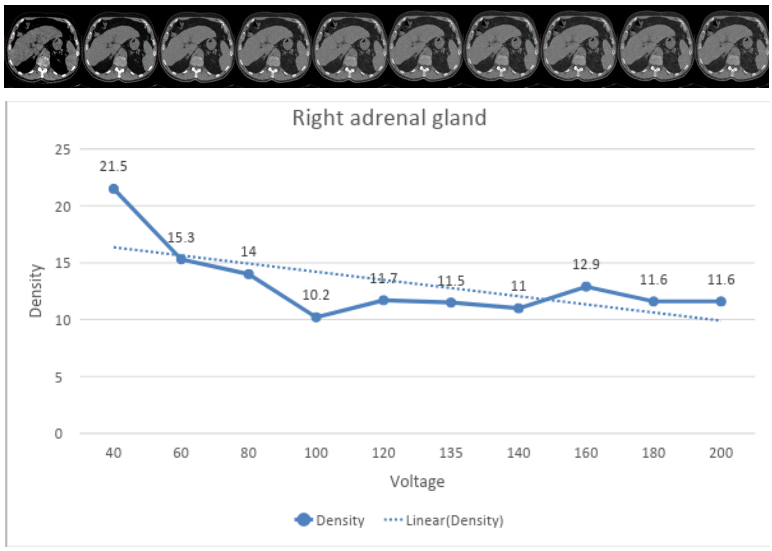

Diagram №10 demonstrates the variation of right adrenal gland density depending on the voltage.

Voltage (kVp)	Density	SD	Min	Max
40	35,5	33,1	-56	111
60	21,7	30,7	-72	91
70	19,8	30,4	-75	87
80	17,7	28,9	-77	84
90	16,2	28,5	-78	82
100	14,8	28,3	-80	81
110	13,7	29,1	-80	85
120	12,8	30,5	-81	87
135	13	30,1	-81	87
140	14,3	29,9	-81	87
160	11,5	29,7	-82	87
180	11,4	29,6	-82	87
200	12,4	30,4	-82	87
200	52,2	25,9	-71	121
Mean value density (HU)		**Standard deviation**	**Maximal density (HU)**	**Minimal density (HU)**
16,51		7,0	35,5	11,4

Table №11 summaries the results of left adrenal gland densities variability.

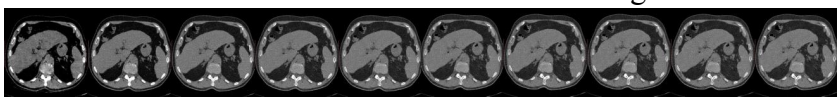

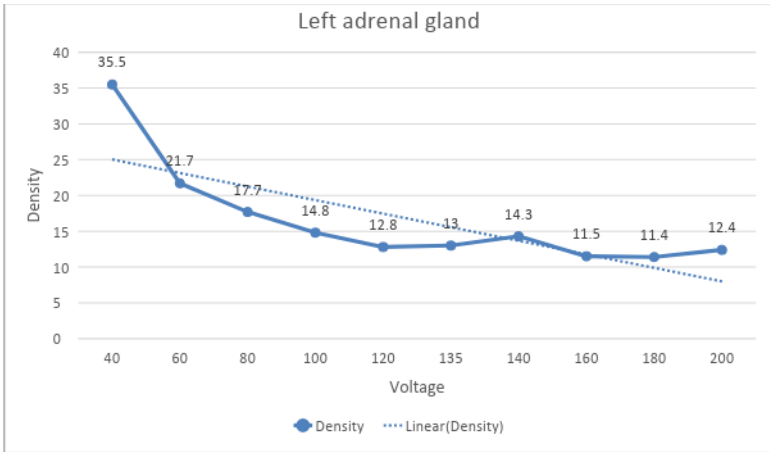

Diagram №11 demonstrates the variation of left adrenal gland density depending on the voltage.

Conclusion

This atlas completes well other established computed tomography anatomy atlas [8] . For the most part, the authors have measured the density of anatomical structures, starting from the highest part of the abdomen and going to the lowest. This study demonstrates the organs and structures densities variability at different voltages. These tables and diagrams can be used in practice for a more accurate interpretation of anatomical structures densities, which measured in images obtained on the different voltage.

References:

- 1. Brenner DJ, Hall EJ. Computed tomography: an increasing source of radiation exposure. N Engl J Med 2007;357(22):2277–2284.
- 2. Schauer DA, Linton OW. National Council on Radiation Protection and Measurements report shows substantial medical exposure increase. Radiology 2009;253(2):293–296.
- 3. Sodickson A, Baeyens PF, Andriole KP, et al. Recurrent CT, cumulative radiation exposure, and associated radiation-induced cancer risks from CT of adults. Radiology 2009;251(1):175–184.
- 4. Mayer C, Meyer M, Fink C, et al. Potential for radiation dose savings in abdominal and chest CT using automatic tube voltage selection in combination with automatic tube current modulation. AJR Am J Roentgenol 2014;203(2): 292–299.
- 5. International Commission on Radiological Protection. Radiological protection in medicine: ICRP publication 105. Ann ICRP 2007;37(6):1–63.
- 6. Effects of the difference in tube voltage of the CT scanner on dose calculation Dong Joo Rhee, Sung-woo Kim, Dong Hyeok Jeong Medical and Radiological Physics Laboratory, Dongnam Institute of Radiological and Medical Sciences, Busan 619-953 Young Min Moon, Jung Ki Kim Department of Radiation Oncology, Dongnam Institute of Radiological and Medical Sciences, Busan 619-953
- 7. McCollough, C. H., Leng, S., Yu, L., & Fletcher, J. G. (2015). Dual- and Multi-Energy CT: Principles, Technical Approaches, and Clinical Applications. Radiology, 276(3), 637–653. doi:10.1148/radiol.2015142631
- 8. Pocket Atlas of Sectional Anatomy, Volume II: Thorax, Heart, Abdomen and Pelvis: Computed Tomography and Magnetic Resonance Imaging 4th Edition, Kindle Edition by Torsten Bert Moeller (Author), Emil Reif (Author)

Learn and upturn

RS-cases

ARTICLE TITLE: Case: asymmetrical temporal bone pneumatization

AUTHORS: Gonchar A.P.1,2, Blokhin I.A.1, Suchilova M.M.2

INSTITUTIONS:

1. Research and Practical Clinical Center of Diagnostics and Telemedicine Technologies, Department of Health Care of Moscow, Russia
2. FSBEI FPE RMACPE MOH, Russia

THESIS:
Goal: To demonstrate a clinical case of asymmetrical temporal bone pneumatization
Materials and methods: A 30-year-old patient with headaches
Results: MRI (magnetic resonance imaging) was performed to the patient and asymmetrical pneumatization of the petrous apex was revealed and further confirmed with CT (computed tomography)
Conclusion: Radiologists need to know anatomical variants of the petrous part of the temporal bone in order to interpret MRI and CT data correctly.
KEYWORDS: Asymmetrical temporal bone pneumatization; computed tomography; magnetic resonance tomography

CORRESPONDING AUTHOR: Gonchar Anna

E-MAIL: anne.gonchar@gmail.com

FOR CITATIONS: Gonchar A.P., Blokhin I.A., Suchilova M. M. - Case: asymmetrical temporal bone pneumatization // Radiology Study. - 2019. - T1., №1. - p. 45-48

Asymmetrical temporal bone pneumatization can be diagnosed with MRI (magnetic resonance imaging) or CT (computed tomography) of the brain in 10% of patients [1]. Such patients often complain about headaches, however, in many cases there are no complaints at all.

It is necessary to remember that this asymmetry is a normal anatomical variation.

The MRI signal of the bone marrow of non-pneumatized petrous apex may frequently be confused with a mass lesion [2, 3]. It must be considered that the signal intensity varies with age: the red bone marrow prevails in children and has intermediate MR signal intensity while in adults it is displaced by fat and has high signal intensity on T1- and T2-weighted images.

In patients with asymmetrical pneumatization high signal intensity on T1, resulting from fat content, may be interpreted as cholesterol granuloma or a soft tissue mass. Usage of several MRI pulse sequences, especially fat suppression, can help to determine a diagnosis. Therefore, CT allows to detect normal bone tissue in non-pneumatized petrous apex [4].

Case study.

A 30-year-old patient with headaches underwent MRI of the brain (pic. 1). The left petrous apex had asymmetric high signal intensity on T1-, T2-WI, T2 Flair and signal dropout on DWI (b=0), which is typical for fat.

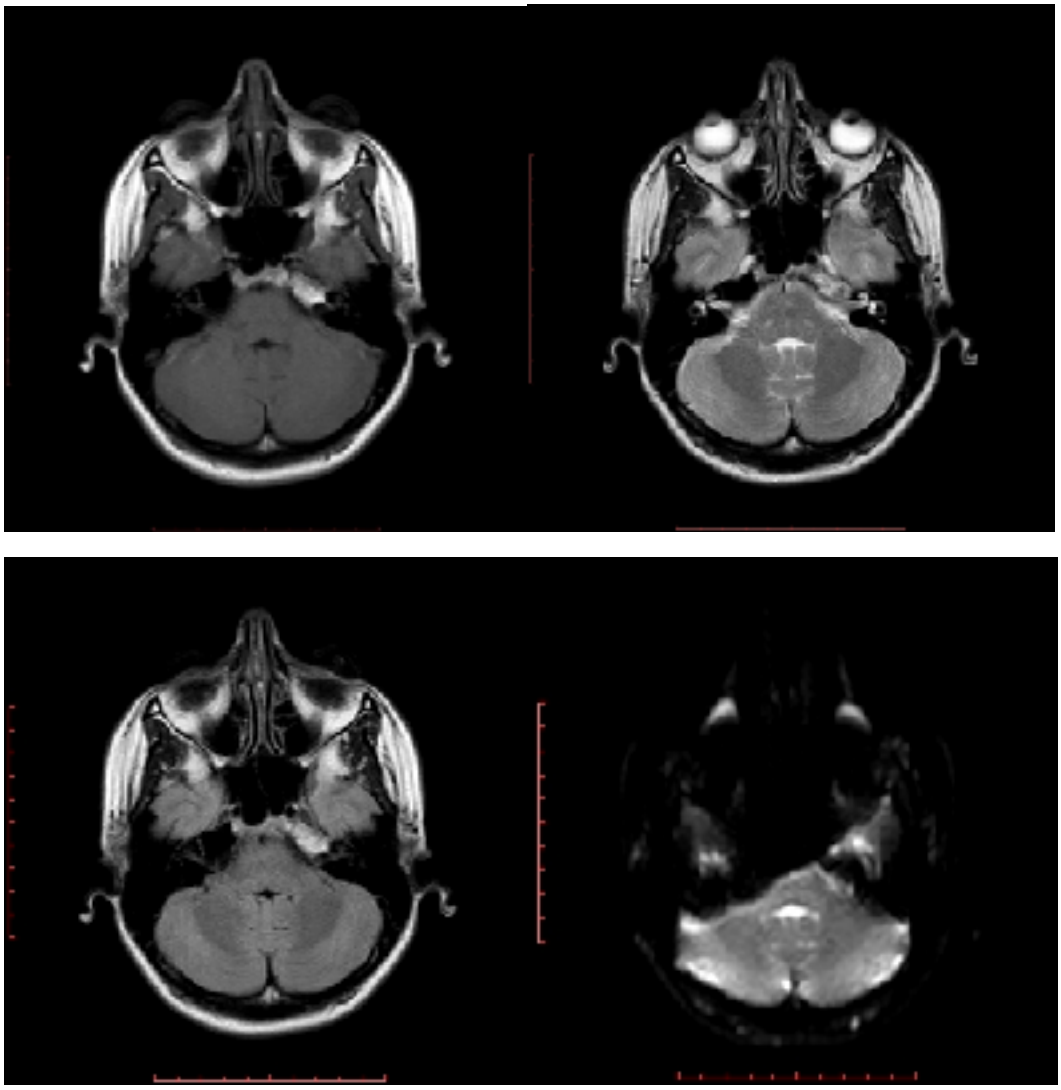

Picture 1. MRI of the brain. Axial view. MRI scans visualise asymmetric high signal intensity of the left petrous apex on T1-WI (a), T2-WI (b) and T2 Flair (c); signal dropout (b=0) on DWI (d).

CT of the brain was performed to the patient in order to confirm asymmetrical pneumatization of the petrous apex (Pic. 2).

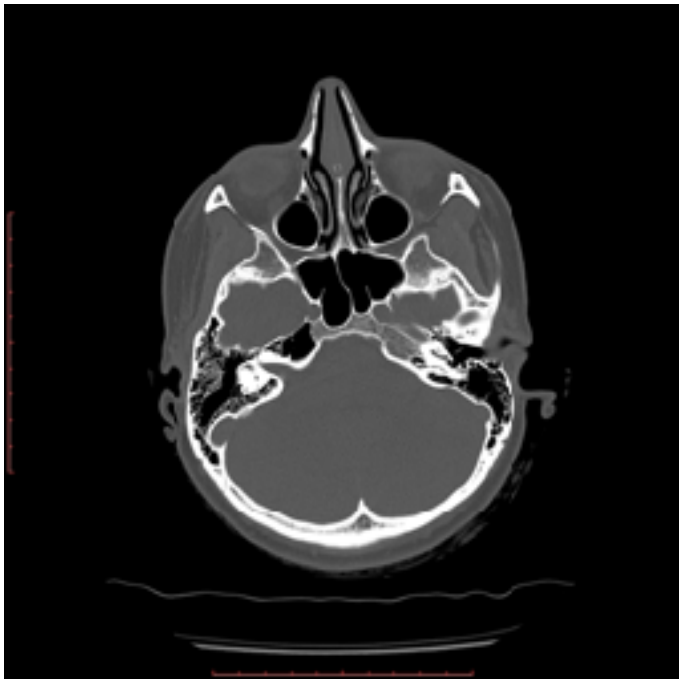

Picture 2. CT scan. Axial view. Asymmetrical pneumatization of the petrous apex. Volume of the air cells is decreased. A normal anatomical variant.

Conclusion.

Radiologists need to know general anatomy and anatomical variants of the petrous part of the temporal bone, which may be confused with pathologies. It will help to avoid extra unnecessary examinations and a possible aggressive approach.

Disclosures.

The authors declare that there is no conflict of interest

References:

1. Connor SE, Leung R, Natas S. Imaging of the petrous apex: a pictorial review. Br J Radiol 2008;81(965):427–435.

2. Isaacson B, Kutz JW, Roland PS. Lesions of the petrous apex: diagnosis and management. Otolaryngol Clin North Am 2007;40(3):479–519.

3. Moore KR, Harnsberger HR, Shelton C, Davidson HC. 'Leave me alone' lesions of the petrous apex. AJNR Am J Neuroradiol 1998;19(4):733–738.

4. Schmalfuss IM. Petrous apex. Neuroimaging Clin N Am 2009;19(3):367–391

Radiologystudy.ru

Learn and upturn

RS-practical part

ARTICLE TITLE: Oncologic PET-CT and SPECT-CT reporting.
AUTHORS: Chernina V.Yu.. Gombolevskiy V.A.1. Dadakina I.S.2
INSTITUTIONS:

1. Research and Practical Clinical Center of Diagnostics and Telemedicine Technologies, Department of Health Care of Moscow, Russia
2. Federal State Autonomous Educational Institution of Higher Education I.M. Sechenov First Moscow State Medical University of the Ministry of Health of the Russian Federation (Sechenov University)

KEYWORDS: PET-CT, SPECT-CT, report, oncology
CORRESPONDING AUTHOR: Chernina Valeriya Yuryevna
E-MAIL: chernina909@gmail.com
FOR CITATIONS: Chernina V.Yu.. Gombolevskiy V.A.1. Dadakina I.S.2 - Oncologic PET-CT and SPECT-CT reporting. // Radiology Study. - 2019. - T1., №1. - p. 50-58

This article presents examples of PET-CT and SPECT-CT study reporting in oncologic practice on the basis of generally accepted recommendations [1-4].

PET-CT whole-body 18F-FDG

Name, Surname:
Gender: female
ID:
Date of birth:
Research date:
The name of the Protocol:
PET/CT device:

Height/body weight:
Radiopharmaceutical, dose:
Location and time of introduction:
Blood glucose level (BG):
Effective dose:
Contrast:
Diagnosis/history:
Objective: Evaluate the treatment response.
Imaging for comparison:

STUDY PROTOCOL: PET study was conducted 60 minutes after the introduction of the radiopharmaceutical, scan area is from the crown to the border of the upper and middle third of the femur. CT-study was conducted in the native phase and post-contrast phase (equilibrium arteriovenous phase).

ARTIFACTS: not detected.

REFERENCE ZONE: SUVmax of the liver - 3,6, SUVmax of the blood pool - 1,9

LYMPH NODE:

- NECK LYMPH NODES: All groups of neck lymph nodes (both sides) are not increased, pathological accumulation of radionuclides is not observed.
- LYMPH NODES OF THE CHEST: All groups of mediastinal lymph nodes are not enlarged, pathological accumulation of radionuclides is not observed. The chest wall lymph nodes and diaphragmatic lymph nodes are not enlarged. Axillary lymph nodes (both sides) are not increased, pathological accumulation of radionuclides is not observed.
- ABDOMEN LYMPH NODES: not enlarged or pathological accumulation of the radionuclides was not observed.
- PELVIS LYMPH NODES: not enlarged or pathological accumulation of the radionuclides was not observed.

- LYMPH NODES EXTERNAL INGUINAL ZONE: not enlarged or pathological accumulation of the radionuclides was not observed.

MUSCULOSKELETAL SYSTEM AND SOFT TISSUES: pathological accumulation of the radiopharmaceutical is not marked in the bones.

- Blastic, lytic lesions are not visualized in the spine.
- Bone structures in the skull are visualized without pathological changes.
- Pathological changes of the bones and soft tissues of the upper extremity are not determined.
- Pathological changes in the bones and soft tissues of the lower extremity pathological changes are not determined.
- Bone structures of the pelvis are visualized without pathological changes.

SIGNIFICANT FINDINGS -

HEAD ZONE: Displacement of the median structures of the brain was not detected.

- CEREBRUM: The gray and white matters are differentiated. Lesions with pathological density in the brain are not visualized.
- LIQUORSTORE SPACE: Subarachnoid spaces and cisterns of the brain are not expanded. Lateral ventricles are symmetric, are not expanded.
- SELLAR REGION: not changed.

SIGNIFICANT FINDINGS -

NECK ZONE: Pathological hyperfixation foci of the radiopharmaceutical in the neck zone are not detected.

- THYROID: Thyroid gland size is not increased, homogeneous structure, hyperfixation foci of the radionuclide are not revealed.
- NASOPHARYNX – without pathologic changes.
- PHARYNX and LARYNX are not deformed, not narrowed. Pear-shaped sinuses are symmetrical. Voice pleats are without pathologic features. The cartilages of the larynx are normal
- SURROUNDING STRUCTURES: salivary glands without pathology.
- NECK VESSELS – without pathological changes.

SIGNIFICANT FINDINGS -

CHEST ZONE: Pathological hyperfixation foci of the radiopharmaceutical in the chest zone are not detected.

- LUNGS: pulmonary parenchyma is normal and adjacent to the chest wall over the entire surface. In both lungs nodules, mass, consolidation are not defined. The walls of the main, large bronchi of both lungs are passable, not thickened, not deformed.
- SOFT TISSUES: soft tissues of the chest are determined without pathological features. The right and left mammary glands are visualized.
- PLEURA and PLEURAL CAVITIES: there is no accumulation of a liquid or a gas in the left and right pleural cavities. The pleura of both hemithoraces is not thickened, not condensed.
- MEDIASTINUM: Mediastinum is located along the median line. The trachea is normal. The esophagus is not changed. The heart is located on the Central line, the

size is not increased. The aorta is not dilated, not calcined. The pulmonary trunk is not dilated. Vena cava is normal. Masses of the upper, anterior, middle, posterior mediastinum are not determined.

- DIAPHRAGM: normal.

SIGNIFICANT FINDINGS -

ABDOMEN and PELVIS ZONES: Pathological hyperfixation foci of the radiopharmaceutical in the abdomen and pelvic zones are not detected.

- LIVER: not increased in size, homogeneous structure. Intra-and extrahepatic ducts, vessels-not expanded.
- GALLBLADDER: not modified, radiopaque concrements are not revealed.
- PANCREAS GLAND: not enlarged, the structure is not changed, duct not dilated.
- SPLEEN: not enlarged, the structure is not changed.
- ADRENAL GLANDS: not enlarged, structurally not changed.
- KIDNEYS and URINARY SYSTEM: there is a physiological distribution of radiopharmaceutical in the kidneys, bladder. The kidneys are normotopic, not enlarged, the structure and density of the parenchyma is not changed. Renal pelvis system is not extended. The ureters aren't dilated. Concretions in the course of the urinary tract is not revealed.
- PELVIC: the bladder is visualized without pathological changes. The uterus and ovaries are determined by normal size, without focal changes. The cecum and the rectum are determined without pathological changes.
- STOMACH: the abdominal part of the esophagus and the stomach are determined without features.
- INTESTINE: the duodenum, loops of the small, haustra of the colon are visualized without pathological changes.
- VESSELS: unremarkable.
- OTHER ORGANS: no free fluid in the abdomen cavity.

SIGNIFICANT FINDINGS -

CONCLUSION:

NM –

OTHER SIGNIFICANT FINDINGS:

PET-CT whole-body 18F-FDG

Name, Surname:
Gender: male
ID:
Date of birth:
Research date:
The name of the Protocol:
PET/CT device:

Height/body weight:
Radiopharmaceutical, dose:
Location and time of introduction:
Blood glucose level (BG):
Effective dose:
Contrast:
Diagnosis/history:
Objective: Evaluate the treatment response.
Imaging for comparison:

STUDY PROTOCOL: PET study was conducted 60 minutes after the introduction of the radiopharmaceutical, scan area is from the crown to the border of the upper and middle third of the femur. CT-study was conducted in the native phase and post-contrast phase (equilibrium arteriovenous phase).

ARTIFACTS: not detected.

REFERENCE ZONE: SUVmax of the liver - 3,6, SUVmax of the blood pool - 1,9

LYMPH NODE:

- NECK LYMPH NODES: All groups of neck lymph nodes (both sides) are not increased, pathological accumulation of radionuclides is not observed.
- LYMPH NODES OF THE CHEST: All groups of mediastinal lymph nodes are not enlarged, pathological accumulation of radionuclides is not observed. The chest wall lymph nodes and diaphragmatic lymph nodes are not enlarged. Axillary lymph nodes (both sides) in all groups are not increased, pathological accumulation of radionuclides is not observed.
- ABDOMEN LYMPH NODES: not enlarged or pathological accumulation of the radionuclides was not observed.
- PELVIS LYMPH NODES: not enlarged or pathological accumulation of the radionuclides was not observed.
- LYMPH NODES EXTERNAL INGUINAL ZONE: not enlarged or pathological accumulation of the radionuclides was not observed.

MUSCULOSKELETAL SYSTEM AND SOFT TISSUES: pathological accumulation of the radiopharmaceutical is not marked in the bones.

- Blastic, lytic lesions are not visualized in spine.
- Bone structures of the skull are visualized without pathological changes.

- The bones and soft tissues of the upper extremity pathological changes are not determined.
- The bones and soft tissues of the lower extremity pathological changes are not determined.
- Bone structures of the pelvis are visualized without pathological changes.

SIGNIFICANT FINDINGS -

HEAD ZONE: Displacement of the median structures of the brain was not detected.

- CEREBRUM: The gray and white matter is differentiated. Lesions with pathological density in the brain is not visualized.
- LIQUORSTORE SPACE: Subarachnoid spaces and cisterns of the brain are not expanded. Lateral ventricles are symmetric, are not expanded.
- SELLAR REGION: not changed.

SIGNIFICANT FINDINGS -

NECK ZONE: Pathological hyperfixation foci of the radiopharmaceutical in the neck zone are not detected.

- THYROID: Thyroid gland in the sizes is not increased, homogeneous structure, hyperfixation foci of radionuclide are not revealed.
- NASOPHARYNX – without pathologic changes.
- PHARYNX and LARYNX not deformed, not narrowed. Pear-shaped sinuses are symmetrical. Voice pleats are without pathologic features. The cartilages of the larynx is normal
- SURROUNDING STRUCTURES: salivary glands is without pathology.
- NECK VESSELS – without pathological changes.

SIGNIFICANT FINDINGS -

CHEST ZONE: Pathological hyperfixation foci of the radiopharmaceutical in the chest zone are not detected.

- LUNGS: pulmonary parenchyma is normal and adjacent to the chest wall over the entire surface. In both lungs nodules, mass, consolidation is not defined. The walls of the main, large bronchi of both lungs are passable, not thickened, not deformed.
- SOFT TISSUES: soft tissues of the chest are determined without pathological features. The right and left mammary glands are visualized normal.
- PLEURA and PLEURAL CAVITIES: there is no accumulation of liquid, gas in the left and right pleural cavities. The pleura of both hemithoraces is not thickened, not condensed.
- MEDIASTINUM: Mediastinum is located along the median line. The trachea is normal. The esophagus is not changed. The heart is located on the Central line, the size is not increased. The aorta is not dilated, not calcined. The pulmonary trunk not dilated. Vena cava is normal. Mass of the upper, anterior, middle, posterior mediastinum are not determined.
- DIAPHRAGM: normal.

SIGNIFICANT FINDINGS -

ABDOMEN and PELVIS ZONES: Pathological hyperfixation foci of the radiopharmaceutical in the abdomen and pelvic zones are not detected.

- LIVER: not increased in size, homogeneous structure. Intra-and extrahepatic ducts, vessels-not expanded.
- GALLBLADDER: not the modified, radiopaque concrements were not revealed.
- PANCREAS GLAND: not enlarged, the structure is not changed, duct not dilated.
- SPLEEN: not enlarged, the structure is not changed.
- ADRENAL GLANDS: not enlarged, structurally changed.
- KIDNEYS and URINARY SYSTEM: there Is a physiological distribution of radiopharmaceutical in the kidneys, bladder. The kidneys are usually located, not increased, the structure and density of the parenchyma is not changed. Renal pelvis system is not extended. The ureters aren't dilated. Concretions in the course of the urinary tract was not revealed.
- PELVIC ORGANS: the bladder is visualized without pathological changes. The prostate gland and seminal vesicles are determined by normal size, without focal changes. Cecum and rectum are defined without pathological changes
- STOMACH: the abdominal part of the esophagus, stomach are determined without features.
- INTESTINE: duodenum, loops of the small, haustra of the colon are visualized without pathological changes.
- VESSELS: unremarkable.
- OTHER ORGANS: no free fluid in the abdomen cavity.

SIGNIFICANT FINDINGS -

CONCLUSION:

NM –

OTHER SIGNIFICANT FINDINGS:

SPECT-CT

Anamnesis: C50.4 Right Breast Cancer T1N0M0.

In April 2015 was radical right mastectomy. Now is hormone therapy.

The radiopharmaceutical - Technetium-99m

Effective dose: 5,0000 mSv

Purpose: The exclusion of metastatic bone disease

Study: bone scan+SPECT-CT

Описание:
The study was performed 120 minutes after the introduction of the radiopharmaceutical.

The physiological distribution of the radiopharmaceutical in the kidneys and bladder is noted.

During the study, the image of the bones of the skeleton of the whole body in the anterior and posterior projections was obtained.

The distribution of the radiopharmaceutical corresponds to the age norm.

Hyperfixation of the radiopharmaceutical characteristic of a specific pathological process, it was not revealed. Degenerative-dystrophic changes revealed of the spine.

The focus of hyperfixation in the anterior part of 6 right ribs is determined, most likely of non-specific character.

Conclusion:
According to bone scan, the presence of radiopharmacy hyperfixation foci typical for the metastatic process was not revealed.

References:

1 - J Nucl Med. 2013 May;54(5):756-61. doi: 10.2967/jnumed.112.112177. Epub 2013 Apr 10. Reporting guidance for oncologic 18F-FDG PET/CT imaging. Niederkohr RD1, Greenspan BS, Prior JO, Schöder H, Seltzer MA, Zukotynski KA, Rohren EM.

2 - Ann Saudi Med. 2011 Jan-Feb;31(1):3-13. doi: 10.4103/0256-4947.75771. 18F-FDG PET/CT imaging in oncology. Almuhaideb A1, Papathanasiou N, Bomanji J.

3 - Diagnostics (Basel). 2018 Mar; 8(1): 9. Published online 2018 Jan 16. doi: 10.3390/diagnostics8010009 PMCID: PMC5871992 PMID: 29337860 Reporting and Handling of Indeterminate Bone Scan Results in the Staging of Prostate Cancer: A Systematic Review Lars J. Petersen,1,2,* Jesper Strandberg,1 Louise Stenholt,3 Martin B. Johansen,4 and Helle D. Zacho1,2

4 - Ann Nucl Med. 2017; 31(10): 719–725. Published online 2017 Sep 1. doi: 10.1007/s12149-017-1202-3 PMCID: PMC5691120 PMID: 28864931 Bone metastases from breast cancer: associations between morphologic CT patterns and glycolytic activity on PET and bone scintigraphy as well as explorative search for influential factors Tsutomu Sugihara,1,5 Mitsuru Koizumi,corresponding author2 Masamichi Koyama,2 Takashi Terauchi,2 Naoya Gomi,3 Yoshinori Ito,4 Kiyohiko Hatake,5 and Naohiro Sata6

ARTICLE TITLE: Anamnestic part before SPECT-CT in oncological practice.

AUTHORS: Nikolaev A.E.1, Shapiev A.N.1, Gombolevskij V.A.1, Blohin I.A.1

INSTITUTIONS:

1. Research and Practical Clinical Center of Diagnostics and Telemedicine Technologies, Department of Health Care of Moscow, Russia

KEYWORDS: SPECT-CT, reporting in oncologic, anamnesis

CORRESPONDING AUTHOR: Nikolayev Aleksandr Evgenyevich

E-MAIL: a.e.nikolaev@yandex.ru

FOR CITATIONS: Nikolaev A.E.1, Shapiev A.N.1, Gombolevskij V.A.1, Blohin I.A.1 - **Anamnestic part before SPECT-CT study in oncological practice.** // Radiology Study. - 2019. - T1., №1. - p. 59-64

Anamnestic part before SPECT-CT study in oncological practice.

Single-photon emission computed tomography (SPECT) combined with standard computed tomography (CT) has a high sensitivity in the detection of multiple metastatic lesions of bone structures [1, 2]. For this study uses usually diphosphonate complexes 99mTc. Most often, the following tumors metastasize into bone structures [3]:

- Breast cancer
- Prostate cancer
- Lung cancer
- Kidney cancer
- Lymphomas
- Neuroblastomas

Metastatic lesions of bone structures are visualized as areas of increased accumulation of radiopharmaceutical (RFP), due to increased osteoblastic activity. With the predominance of osteolytic activity, which is much less common osteoblastic foci, it is possible to meet false negative results, occurring mainly in thyroid cancer and multiple myeloma.
High sensitivity SPECT-CT is associated with low specificity as high metabolic activity is caused by the following processes [1]:

- Benign tumor process
- Primary malignant tumor process
- Secondary malignant tumor process
- Inflammatory process
- Degenerative changes

Based on the above facts, it is necessary to carefully collect the history before the examination according to the algorithm, which is presented below in the form of written surveys:
The questionnaire before performing the bone scan [1].
Surname First Name:_____
Date of birth:_____
Weight (kg)_____ Height (cm)_____

Phone:_____
Phone relatives:_____
Phone for communication in case of emergency:_____
Date of future doctor's appointment:_____
The reason for this study:_____
_____

You previously performed bone scan? YES NO
If so, when and where?_____
Did you bring any previous x-rays, CT scans or MRI scans? YES NO
Have you done any other radionuclide tests today? YES NO
Earlier Your physicians have diagnosed You with one of the following pathologies?
- Osteoarthritis YES NO
- Rheumatoid arthritis YES NO
- Other pathology of the musculoskeletal system YES NO
(if YES-be sure to remember and describe)
_____
_____
_____

How long have you had bone pain?_____
Cause of pain:_____
Localize the pain_____
Did you have injuries, fractures, falls? YES NO
(if YES-be sure to remember, describe) _____
_____
_____

Have you had any injuries, fractures, falls RECENTLY? YES NO
(if YES-be sure to remember and describe)

_____

_____

Do you see a dentist? YES NO
If Yes, write the date of the last visit_____
If Yes, write the date, the reason for the visit_____

_____

Have you performed surgery (removal of the prostate gland, breast surgery, spinal surgery, heart surgery, etc.) YES NO
(if YES - be sure to remember and describe)

_____

_____

If you have a oncologic history (cancer)? YES NO
(if YES - be sure to remember and describe)

_____

_____

Do you take any medications related to your current condition?
YES NO
(if YES - be sure to remember and describe)

_____

_____

_____

Did you perform intra-articular injections? YES NO
(if YES - be sure to remember and describe)

_____

_____

_____

Questions for women:
If the probability that you are pregnant? YES NO
Are you currently breastfeeding? YES NO
Please highlight the areas in the diagram below that are painful (if appropriate):

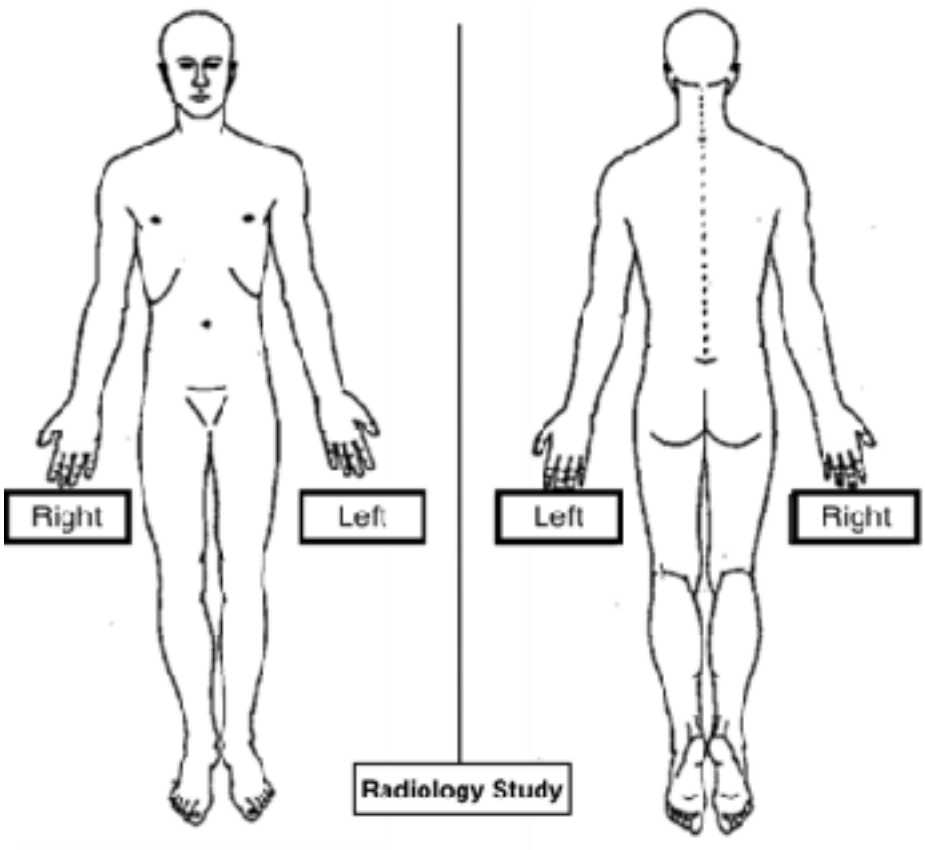

I have read this form, understand the purpose and risks of the study and agree to conduct the study:

Patient's first Name:_____

Patient signature (or guardian signature): _____

References:

[1] - Indian J Nucl Med. 2016 Jul-Sep; 31(3): 185–190. doi: 10.4103/0972-3919.183605 PMCID: PMC4918480 PMID: 27385887 Metastatic mimics on bone scan: “All that glitters is not metastatic” Archi Agrawal, Nilendu Purandare, Sneha Shah, and Venkatesh Rangarajan

[2] - Nucl Med Commun. 2011 Dec;32(12):1194-200. doi: 10.1097/MNM.0b013e32834bd82e. Differential diagnostic value of single-photon emission computed tomography/spiral computed tomography with Tc-99m-methylene diphosphonate in patients with spinal lesions. Zhang Y1, Shi H, Gu Y, Xiu Y, Li B, Zhu W, Chen S, Yu H.

[3] - Oncol Rev. 2017 Mar 3; 11(1): 321. Published online 2017 May 9. doi: 10.4081/oncol.2017.321 PMCID: PMC5444408 PMID: 28584570 Bone Metastases: An Overview Filipa Macedo,1 Katia Ladeira,2 Filipa Pinho,2 Nadine Saraiva,1 Nuno Bonito,1 Luisa Pinto,2 and Francisco Goncalves2

ARTICLE TITLE: Assessment of cardiotoxicity in patients with breast cancer (AJCC - IV), according to PET-CT.

AUTHORS: Nikolaev A.E.1, Suchilova M. M.2, Korkunova O. A.2, Gombolevskij V.A.1, Blohin I.A.1

INSTITUTIONS:
1. Research and Practical Clinical Center of Diagnostics and Telemedicine Technologies, Department of Health Care of Moscow, Russia
2. FSBEI FPE RMACPE MOH, Russia

KEYWORDS: cardiotoxicity, PET-CT, breast cancer

CORRESPONDING AUTHOR: Nikolayev Aleksandr Evgenyevich

E-MAIL: a.e.nikolaev@yandex.ru

FOR CITATIONS: Nikolaev A.E.1, Suchilova M. M.2, Korkunova O. A.2, Gombolevskij V.A.1, Blohin I.A.1 - Assessment of cardiotoxicity in patients with breast cancer (AJCC - IV), according to PET-CT. // Radiology Study. - 2019. - T1., №1. - p. 65-70

Breast cancer (BC) is one of the most common malignant tumors and a serious healthcare problem all over the world [1].

The incidence of breast cancer increases with age, starts at the age of 40 and reaches a peak between ages of 60-65. The incidence rates of breast cancer in the USA amounts to 32% of all newly diagnosed cases of cancer in women. High rates of morbidity and mortality due to BC take this disease to the first place in oncologic structure in Russia. The average five-year survival rate is 55%.

The main radiologic imaging methods for detecting breast cancer include mammography, which is used for screening, ultrasound and breast MRI.

MRI is the most sensitive and specific way to evaluate regional lymphatic nodes and to determine the T (tumor)- stage. Modern fast protocols allow to perform MRI with contrast in less than 10 minutes. For this reason many authors suggest using MRI for breast cancer screening.

At the present time, scintigraphy with SPECT-CT (single photon emission computed tomography combined with computed tomography) is used in many clinics for NM (Nodule, Metastasis)-staging. Many authors also suggest using whole-body MRI for NM-staging, but this method is difficult to reproduce, thuswise 18F-FDG PET-CT (18F-flurodeoxyglucose positron emission tomography-computed tomography) still remains the method of choice. PET-CT with FDG is used for both NM-staging and tumor response evaluation.

Methods of breast cancer treatment include:

- Surgery
- Radiation therapy
- Hormonal therapy
- Chemotherapy
- Targeted therapy

Drug therapy includes neoadjuvant and adjuvant therapy. It is important to give special consideration to cardiotoxicity, since chemotherapy and targeted therapy are used widely and often cause this adverse reaction [2]. Cardiotoxicity is a condition when there is a pathological changes of cardiovascular system of cancer patients associated with drug therapy.

Cardiovascular events according to chemotherapy regimens are provided below [3].

Drugs	Cardiovascular events
Anthracyclines	Left ventricular failure, heart failure, myocarditis, arrhythmia
5-Flourocil	Ischemic heart disease, heart failure, pericarditis, cardiogenic shock
Taxanes	Sinus bradycardia, ventricular tachycardia, atrioventricular block, heart failure, ischemic heart disease
Cyclophosphamide	Heart failure (neurohumoral activation), mitral regurgitation
Trastuzumab	Heart failure, left ventricular failure, arrhythmia
Tamoxifen	Thromboembolism, disorders of cholesterol metabolism
Bevacizumab	High blood pressure, thromboembolism
Selective COX-2 inhibitors	Thromboembolism

Suter и Ewer offered to classify all the cytostatics and targeted drugs according to the types of cardiovascular damages.
I type - irreversible myocardial dysfunction due to cardiomyocyte death (e.g., anthracyclines). The degree of myocardial damage depends on cumulative dose.
II type - reversible myocardial dysfunction due to mitochondrial and protein damages. This type is typical for trastuzumab and does not depend on cumulative dose [2].

Detection of cardiotoxicity include:

- Medical history data (patient's complaints, physical examination, arterial blood pressure)
- Laboratory diagnostics (troponin test)
- Instrumental examination (electrocardiography (ECG) - QT interval)
- Echocardiography (EchoCG) (evaluation of the ejection fraction)
- Radiologic imaging methods (CT, SPECT, ets.)

Now EchoCG is the most commonly used method for evaluation chemotherapy effects on the cardiovascular system. The left ventricular ejection fraction should be carefully measured. Reduction of the ejection fraction is detected on standard EchoCG only when the compensatory mechanisms are not working. It also should be remembered that the left ventricular ejection fraction does not always associated with cardiotoxicity and can be observed in other diseases. EchoCG comparison of the ejection fraction before and after the beginning of the therapy is not always adequate because this is an operator-dependent method and digital archives are not provided in the majority of clinics.

After EchoCG cardiotoxicity is estimated with MRI for various types of pericarditis, cardiomyopathy, valve pathology, when CT is used for coronary artery evaluation and pericarditis (figure 1) [4].
Such methods of radionuclide diagnostics as SPECT and PET investigate the myocardial ability to capture labelled particles and caracterise neuronal coherence. Evaluation of the absorption and further release of the radiopharmaceutical agent allows to estimate adrenergic function (the slower the release, the greater the chance of heart failure developing).
Despite all mentioned methods uptake changes can be indicated with standard 18F-FDG PET-CT performed for restaging.

Chaitanya Borde and co-authors suggest establishing **3 patterns** of myocardial changes in dynamics on whole body FDG PET-CT:
1 - no changes - not associated with cardiotoxicity;
2 - increase and **3 - decrease** of metabolic activity in the cardiac region - associated with cardiotoxicity (pic. 1 and pic. 2) [5].

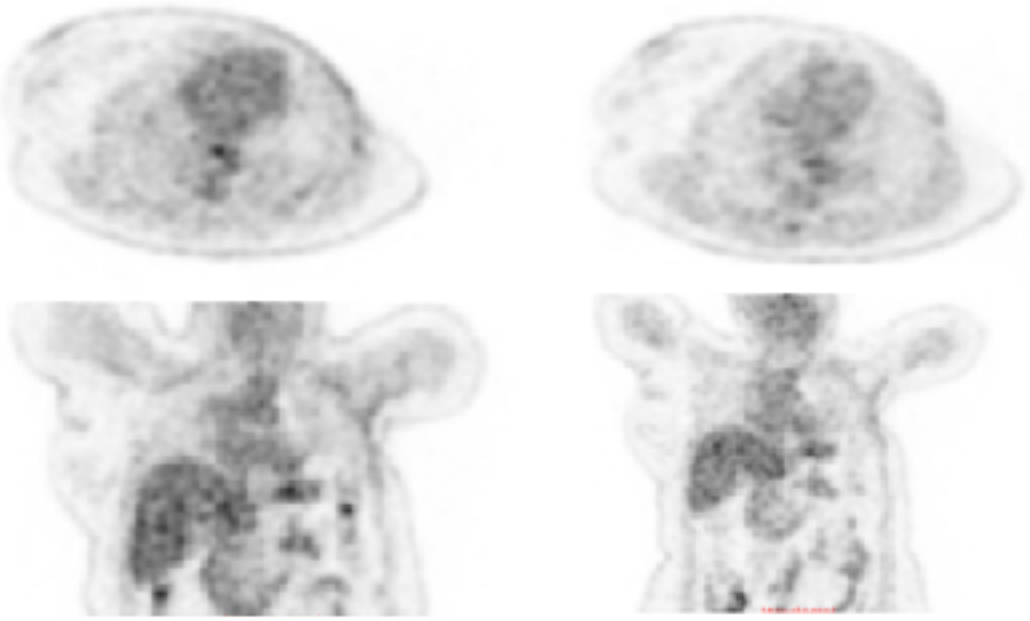

Picture 1. The decrease of cardiac FDG activity after 6 months of chemotherapy.

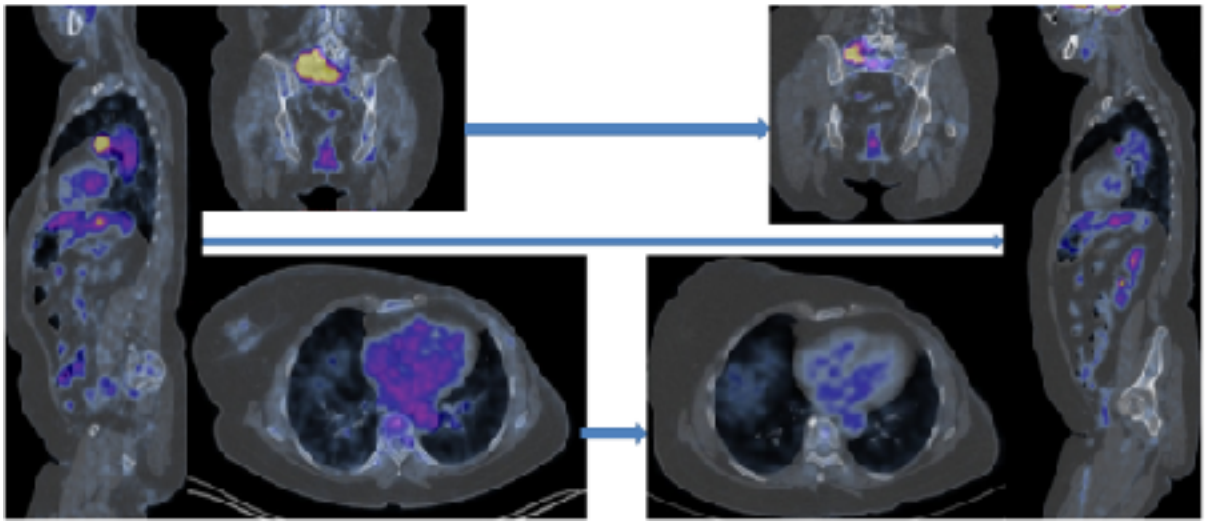

Picture 2. Partial response of underlying disease.

The decrease of metabolic activity is visualised in the cardiac region. This patient needs further ultrasound examination for ejection fraction evaluation due to a high risk of cardiotoxicity development.

Joanna Wykrzykowska and co-authors showed that not only myocardial uptake of the radiopharmaceutical agent can be visualized, but also the local increase of activity is possible to detect (e.g., along the left anterior descending artery) [6].

Close attention should be paid to the ejection fraction measured with EchoCG, ECG and the troponin test according to the case management procedures, that was recommended by European Society for Medical Oncology for patients with cardiotoxicity. However, the case

management contains a few information about other diagnostic procedures, especially radiologic imaging methods [2].

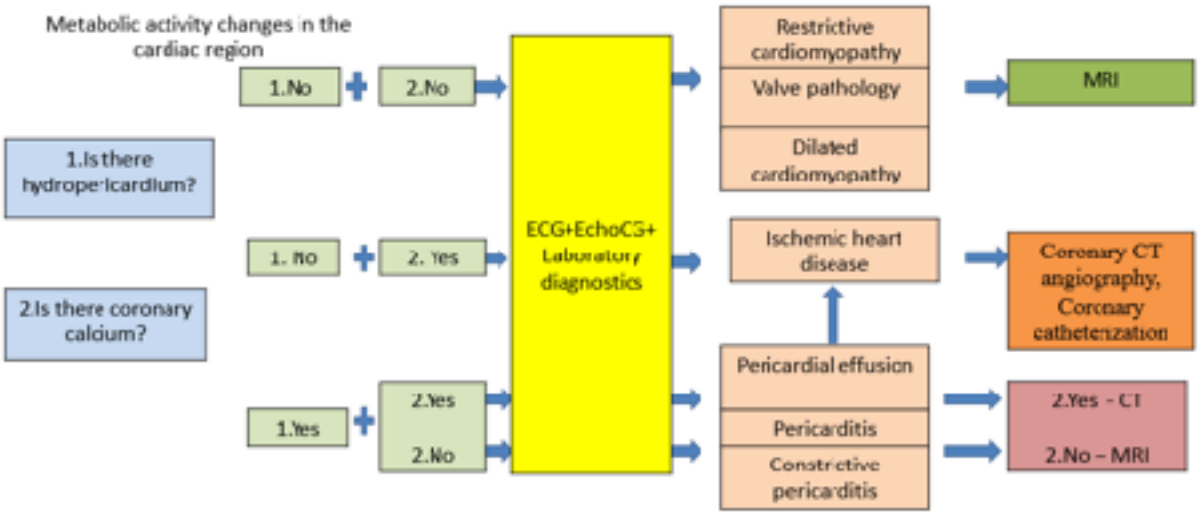

Figure 1. There are 3 patterns of activity changes in the myocardial region: with no changes, increased and decreased (the last two are associated with cardiotoxicity).
Not only metabolic activity changes, but also additional findings require close attention. Such findings as hydropericardium and coronary calcium can help to determine case management procedures.

Conclusion:

Cardiotoxicity according to the data of the oncologic FDG PET-CT isn't studied well yet and for this reason it is of interest for scientific research. However, it's important to pay close attention at the changes in cardiac FDG activity when PET-CT scans are compared over time.

References:

[1] - Siegel R, Naishadham D, Jemal A. Cancer statistics, 2012. CA Cancer J Clin. 2012 Jan-Feb;62 (1):10–29.

2] - Seliverstova D. V.. Evsina O. V. Kardiotoksichnost khimioterapii. Serdtse: zhurnal dlya praktikuyushchikh vrachey. 2016;15 (1):50–57 DOI: 10.18087 / rhj.2016.1.2115

[3] - Chemotherapy-induced Cardiotoxicity Maria FLORESCUa,b; Mircea CINTEZAa,b; Dragos VINEREANUa,b a Emergency University Hospital, Bucharest, Romania b ”Carol Davila” University of Medicine and Pharmacy, Bucharest, Romania

[4] - Cardiac Complications of Oncologic Therapy1 Christopher M. Walker, MD • David A. Saldaña, MD • Gregory W. Gladish, MD • Demetrius L. Dicks, MD • Gregory Kicska, MD, PhD • Lee M. Mitsumori, MD, MS • Gautham P. Reddy, MD

[5] - Chaitanya Borde, Purushottam Kand, Sandip Basu Enhanced myocardial fluorodeoxyglucose uptake following Adriamycin-based therapy: Evidence of early chemotherapeutic cardiotoxicity? World J Radiol. 2012 May 28; 4(5): 220–223. doi: 10.4329/wjr.v4.i5.220

[6] - Journal Nuclear Medicine - 2009 Apr;50(4):563-8. doi: 10.2967/jnumed.108.055616. Epub 2009 Mar 16. Imaging of inflamed and vulnerable plaque in coronary arteries with 18F-FDG PET/CT in patients with suppression of myocardial uptake using a low-carbohydrate, high-fat preparation. Wykrzykowska J1, Lehman S, Williams G, Parker JA, Palmer MR, Varkey S, Kolodny G, Laham R.

Radiologystudy.ru

Learn and upturn

RS-Tendencies

ARTICLE TITLE: UI-RADS (Uterus Imaging Reporting and Data System)
AUTHORS: Dadakina I.S., Lbova O.A.2. Gombolevskiy V.A.3.
INSTITUTIONS:

1. Federal State Autonomous Educational Institution of Higher Education I.M. Sechenov First Moscow State Medical University of the Ministry of Health of the Russian Federation (Sechenov University)
2. Pirogov Russian National Research Medical University (RNRMU)
3. Research and Practical Clinical Center of Diagnostics and Telemedicine Technologies, Department of Health Care of Moscow, Russia
KEYWORDS: Uterine sarcoma, UI-RADS, Uterus Imaging Reporting and Data System
CORRESPONDING AUTHOR: Dadakina Iya Sergeyevna
E-MAIL: iya_dadakina@mail.ru
FOR CITATIONS: Dadakina I.S., Lbova O.A.2. Gombolevskiy V.A.3. - UI-RADS (Uterus Imaging Reporting and Data System) // Radiology Study. - 2019. - T1., №1. - p. 72-73

Uterine sarcoma is a rare disease of the uterus body and accounts for about 5% of all uterine tumors and 1% of gynecological diseases. This pathology is detected more often in the postmenopausal period.

Types of uterine sarcoma:

- leiomyosarcoma
- endometrial stromal sarcoma
- undifferentiated sarcoma

Clinical symptoms are variable and depend on the histological type of sarcoma. Manifestations of this disease are non-specific, so the Centers for disease control and prevention (CDC) of the United States proposed to perform 1 every 2 years of preventive ultrasound examinations (ultrasound) of women aged 35 to 65 years for the detection and characterization of focal uterine changes.

The system is similar to the well-known BI-RADS (reporting breast imaging and system data) and is called UI-RADS (Uterus Imaging Reporting and Data System).

Classification UI-RADS:

- UI-RADS 0: Need further imaging because of poor-quality study
- UI-RADS 1: Normal uterus, no masses
- UI-RADS 2: Uterine tumor present, benign (single tumor, < 5 cm, no necrosis, echogenicity consistent with benign fibroid)
- UI-RADS 3: Uterine tumor(s) present, cannot be classified as most likely benign (multiple tumors, size 5-10 cm, no central necrosis, indeterminate echogenicity)
- UI-RADS 4: Uterine tumors(s) present, concerning findings for malignancy (multiple tumors, size > 10 cm, < 10% central necrosis present, indeterminate echogenicity)
- UI-RADS 5: Uterine tumor(s) present, most likely malignant (multiple tumors, size > 10 cm, > 10% central necrosis, echogenicity consistent with malignancy)
- UI-RADS 6: Uterine tumor(s) present, previously established malignancy present

Recommendations UI-RADS :

- UI-RADS 0: Repeat imaging
- UI-RADS 1: Routine screening
- UI-RADS 2: Follow-up imaging at one year; if unchanged, proceed with routine imaging follow-up. If growing > 50% in one year, upgrade to UI-RADS 3. If clinical symptoms require myomectomy, perform with intraoperative biopsy to establish a reasonable assurance of benignity before surgically violating the uterine capsule. If clinical symptoms require total uterine resection, perform without tumor disruption.
- UI-RADS 3: Follow-up imaging at six months and one year; if unchanged, proceed with routine imaging follow-up. A stable UI-RADS 3 downgrades to UI-RADS 2. If growing > 50% in one year, upgrade to UI-RADS 4. If clinical symptoms require myomectomy, perform with intraoperative biopsy to establish a reasonable assurance of benignity before surgically violating the uterine capsule. If clinical symptoms require total uterine resection, perform without tumor disruption.
- UI-RADS 4: Establish clinical concordance (i.e., severe bleeding, anemia, pelvic pressure, dyspareunia, urinary frequency), measure LDH level, and perform abdominal CT or MRI. Perform screening chest CT. In "concordant" cases, proceed with an oncologically safe uterine resection as soon as possible, given the high likelihood of malignancy. If the woman is interested in maintaining her fertility, myomectomy can be considered only after tissue biopsy provides a reasonable assurance of benignity. In "discordant" cases, offer UI-RADS 4 patients an oncologically safe uterine resection or, if the patient prefers to maintain her uterus for family planning reasons, perform a biopsy to establish a reasonable assurance of benignity.
- UI-RADS 5: Establish clinical concordance. Perform alternative imaging to better characterize the tumor(s). Perform a staging chest CT. Proceed to an oncologically safe uterine resection. Do not offer myomectomy.
- UI-RADS 6: Patient under direct care of a gynecologic oncologist and medical oncologist.

References:

1 - Article by Hooman Noorchashm MD, PhD - https://medium.com/@noorchashm/an-open-letter-to-the-american-college-of-radiology-on-the-dangerous-deficit-in-radiological-46bfc9f02382

Radiologystudy.ru

Learn and upturn

RS-TEST

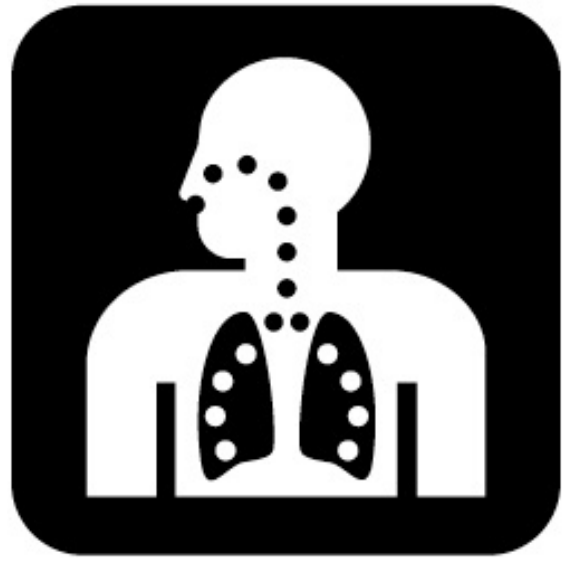

1. What caused the changes of the clivus on these MRI images?

1. meningioma
2. inflammation in the petrous part of the temporal bone
3. chordoma
4. asymmetric pneumatization petrous apex

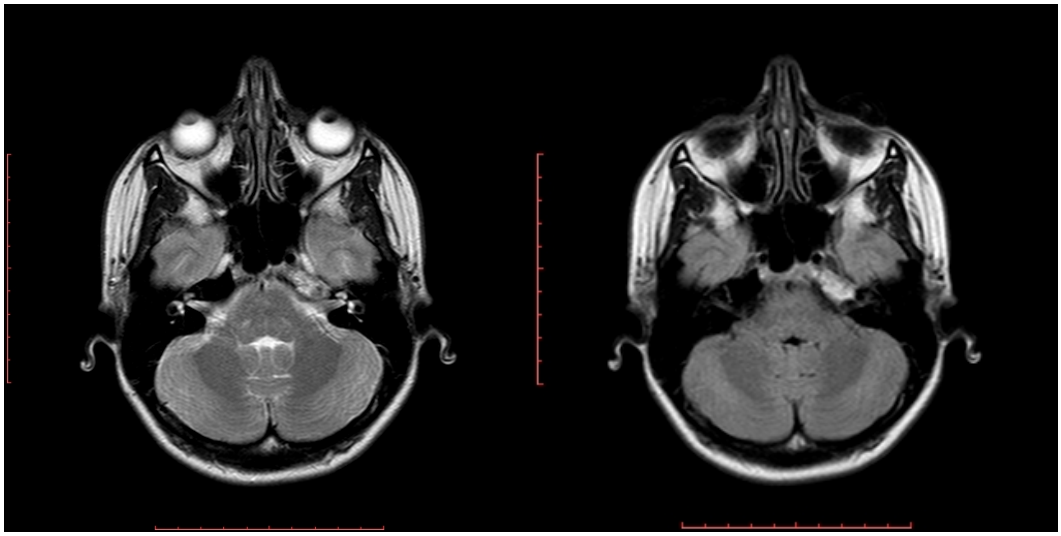

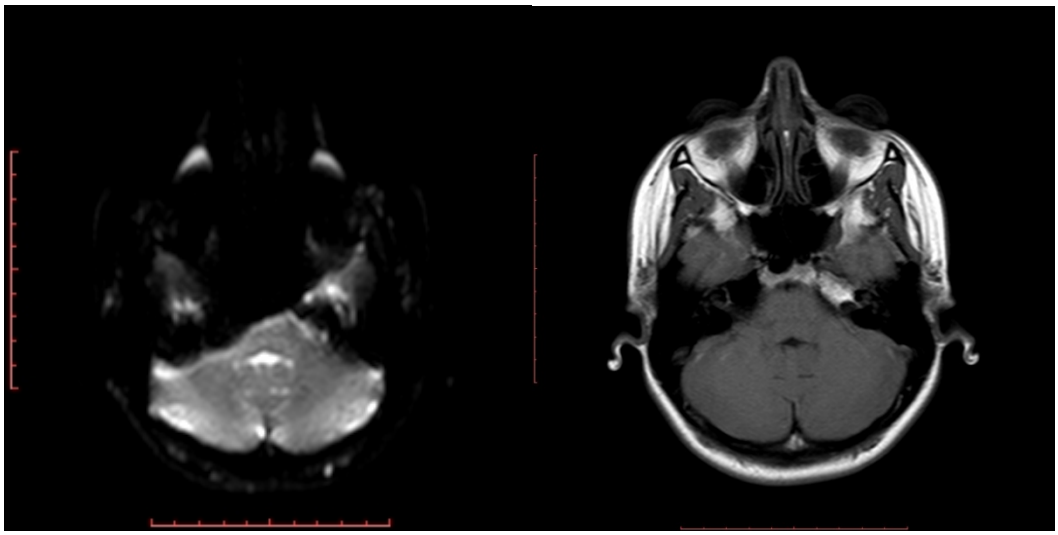

2. What SUV values witness of a probability of the thyroid malignancy?

1. 0-2.5
2. 2.5-5
3. 5-7.5
4. 7.5-10
5. All answers are correct

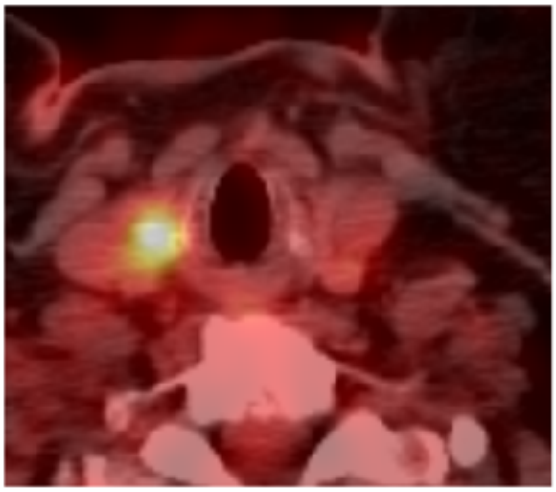

3. What cases presume surgery when dealing with aneurysm of thoracic aorta? (Select the correct answers)

1. Aorta grows at a rate of roughly 0.3 cm per year
2. Aorta grows at a rate of roughly 0.5 cm per year
3. The initial aortic diameter greater than 5,5 cm (on initial examination)
4. The initial aortic diameter greater than 4,5 cm (on initial examination)

4. How does the bone density change during CT with increasing voltage?

1. Increase
2. Same
3. Decrease

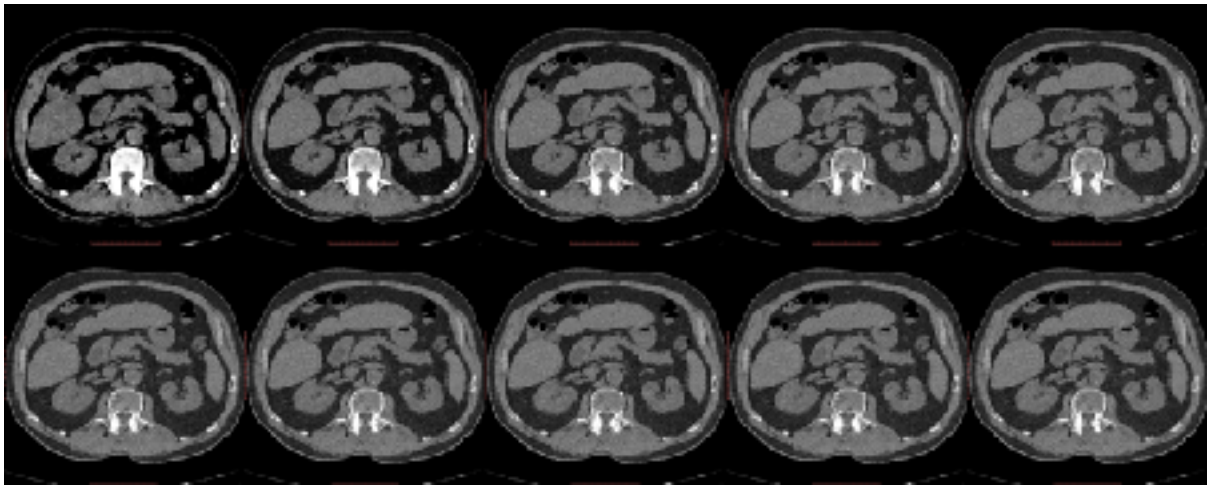

5. How does the spleen density change during CT with increasing voltage?

1. Increase
2. Same
3. Decrease

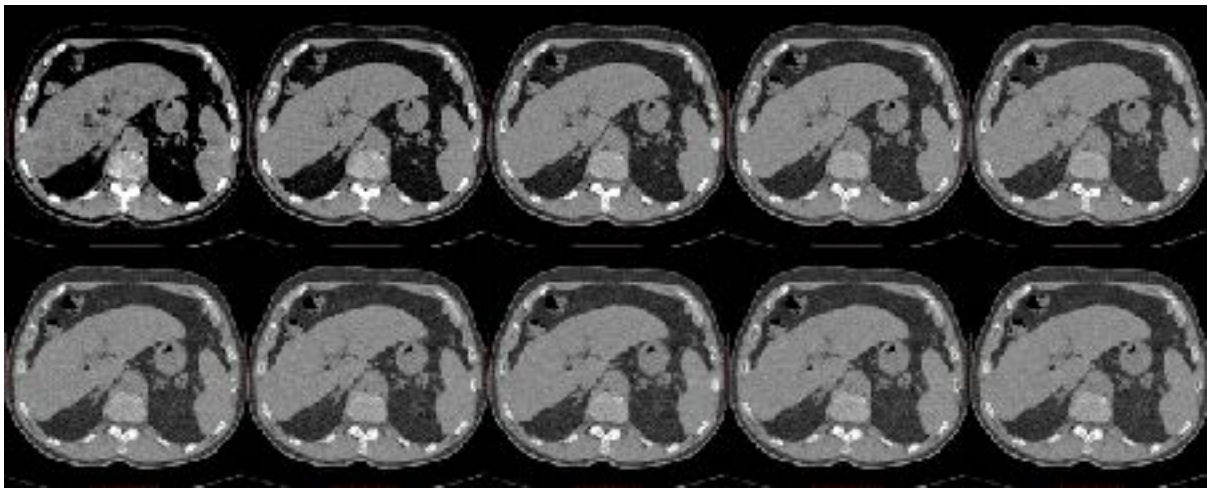

6. Bone metastasis is more likely with cancers such as:

1. Breast
2. Liver
3. Prostate
4. Lung
5. Kidney

7. Which pattern of aortic calcination is characterized for atherosclerosis?

1. Circumferential calcification,
2. Confluent calcification,
3. Patchy calcification.

Answers:

1 - 4

2 - 5

3 - 2, 3

4 - 3

5 - 1

6 - 1, 3, 4, 5

7 - 3

Test prepared by Anna Pavlovna Gonchar - the researcher of "Research and Practical Clinical Center of Diagnostics and Telemedicine Technologies, Department of Health Care of Moscow, Russia".

Radiologystudy.ru

Learn and upturn

RS-April 2019